Technical Report Documentation Page

1. Report No. Aurora Project 2016-03	2. Government Accession No.	3. Recipient's Catalog No.	
4. Title and Subtitle Optimal RWIS Sensor Density and Location – Phase II		**5. Report Date** November 2019	
		6. Performing Organization Code	
7. Author(s) Simita Biswas, Tae J. Kwon, Shuoyan Xu, and Liping Fu		**8. Performing Organization Report No.** Aurora Project 2016-03	
9. Performing Organization Name and Address Department of Civil & Environmental Engineering, University of Alberta 9211-116 Street NW, Edmonton, Alberta, Canada T6G 1H9		**10. Work Unit No. (TRAIS)**	
		11. Contract or Grant No.	
12. Sponsoring Organization Name and Address Aurora Program Iowa Department of Transportation 800 Lincoln Way Ames, Iowa 50010	Federal Highway Administration U.S. Department of Transportation 1200 New Jersey Avenue SE Washington, DC 20590	**13. Type of Report and Period Covered** Final Report	
		14. Sponsoring Agency Code TPF SPR 72-00-0003-042	

15. Supplementary Notes

Visit www.aurora-program.org for color pdfs of this and other Aurora Pooled Fund research reports.

16. Abstract

Preventing weather related crashes is a significant part of maintaining the safety and mobility of the travelling public during winter months. A Road Weather Information System (RWIS) is a combination of advanced technologies that collect, process, and disseminate road weather and condition information. This information is used by road maintenance authorities to make operative decisions that improve safety and mobility during inclement weather events. Many North American transportation agencies have invested millions of dollars to deploy RWIS stations to improve the monitoring coverage of winter road surface conditions. However, the significant costs of these systems motivate governments to develop a framework to optimize the spatial design of the RWIS network. The design of these networks often varies by region, and it remains an unresolved question what should be the optimal density and location of a RWIS network to provide adequate monitoring coverage of a given region.

To fill this gap, this project is aimed at developing a methodology for optimizing the density and location of a RWIS network for a given region based on its topographic and weather characteristics. A series of geostatistical spatiotemporal semivariogram models were constructed and compared using topographic position index (TPI) and weather severity index (WSI) to measure relative topographic variation and weather severity, respectively. Specifically, this project considered the nature of spatiotemporally varying RWIS measurements by integrating larger case studies and examining two analysis domains: space and time. The study area captured varying environmental characteristics, including regions with flatland or varied terrain and different severities of winter weather. The optimal RWIS density and location for different topographic and weather severity regions were determined using spatiotemporal semivariogram parameters. Output of this study revealed a strong dependency of optimal RWIS density on topographic and weather characteristics of a region. Moreover, this study suggests that RWIS data collected from a specific region can be used to estimate the number of stations required for regions with similar zonal characteristics. The proposed method will provide decision makers with a tool they need to develop a long-term RWIS implementation plan.

17. Key Words road weather information systems (RWIS), space time kriging, geostatistics, location allocation, density optimization		18. Distribution Statement No restrictions.	
19. Security Classification (of this report) Unclassified.	**20. Security Classification (of this page)** Unclassified.	**21. No. of Pages** 99	**22. Price** NA

Department of Civil & Environmental Engineering

University of Alberta

Optimal RWIS Sensor Density and Location – Phase II

Final Report

December 2019

Aurora Project 2017 – 19

http://www.aurora-program.org

*Tae J. Kwon, Ph.D., Assistant Professor
*Simita Biswas, Graduate Research Assistant
*Shuoyan Xu, Graduate Research Assistant
&
**Liping Fu, PhD., P.Eng.

*Department of Civil and Environmental Engineering
University of Alberta, Edmonton, AB, Canada, T6G 2W2
Tel: +1(780) 492-6121, Fax: +1(780) 492-0249
Email: tjkwon@ualberta.ca

**TransOptimum Technology Inc.
526 Birchlead Walk, Waterloo, ON., Canada, N2T 2W5
Tel: +1(519) 591-9933
Email: lfu6688@gmail.com

Table of Content

List of Figures

List of Tables

EXECUTIVE SUMMARY

The prevention of weather-related road crashes continues to be a vital and challenging issue particularly for countries in cold regions. As an important part of modern transportation engineering, Intelligent Transportation Systems (ITS) plays an essential role in our everyday life by improving transportation safety and mobility. Road Weather Information System (RWIS), a critical piece of ITS infrastructure, is a combination of advanced technologies that collect, process, and distribute road weather and condition information. RWIS information is used by road maintenance agencies to make operative decisions during winter season to ensure traffic safety and mobility of the travelling public. For this reason, many North American transportation agencies have invested millions of dollars to deploy additional RWIS stations onto their road network to improve the winter road monitoring coverage. Because of the significant cost associated with RWIS station installation, it is essential to develop a RWIS network planning and deployment guideline. To address such challenging issues and improve the generalization potential, this project investigated the dependency of optimal RWIS densities to readily available zonal characteristic data with a need for a long-term strategic RWIS deployment plan. The topographic characteristics and weather severity of the associated study area were selected as zonal classification standards and used for developing optimal RWIS density guidelines. Main findings and key contributions of this project are summarized below:

Topographic Position Index (TPI)

The topography based zonal classification was conducted using the topographic position index (TPI), which defines a relative topographical variation of an area of interest and its neighborhood. The TPI value of each point is calculated by comparing the elevation of every point with the average elevation of a user defined neighborhood region. A higher TPI value indicates a varied topographic region, while a lower TPI value indicates a flatland area. According to the TPI values, the study area was classified into three different landform groups: flatland area, hilly area and mountainous area.

Weather Severity Index (WSI)

The weather severity based zonal classification was conducted using an integrated winter weather measure - winter severity index (WSI), which provides a numerical estimate of weather severity

using annual average snowfall accumulation and duration, annual duration of blowing snow, and annual duration of freezing rain. A WSI map of the United States generated by Meridian Environmental Technology was adopted for this study for weather severity classification. According to the WSI values, the study area is categorized into four WSI based classes: less, moderate, high, and extremely high severe weather zones. Generally speaking, weather severity increases from the southern to the northern parts of the study area.

Investigation of Spatiotemporal Characteristics of Road Weather and Topographic Factors
Geostatistical spatiotemporal semivariogram modeling was used in this study to incorporate both spatial and temporal variations of various weather variables monitored by RWIS. A semivariogram measures the similarity between two measurements as a function of separation distance. Larger autocorrelation ranges indicate greater spatiotemporal continuity of RWIS measurements and vice versa. The findings suggest that flatland areas with less-varied weather were shown to have a greater continuity range than hilly or mountainous regions and more severe weather regions; thus, comparatively fewer RWIS stations were needed to provide a certain level of monitoring coverage.

Development of Region-wide RWIS Deployment Strategies
An innovative optimization framework was developed and enhanced to optimize the spatial design of a regional RWIS network by incorporating the ultimate use of RWIS information for spatiotemporal inference as well as traffic distribution. The problem was formulated on a basic premise that data from individual RWIS in a region should collectively be used to maximize their overall monitoring quality. The spatial simulated annealing (SSA) algorithm was employed to solve the optimization problem in an efficient manner. The optimization was run for two distinct scenarios – 1) all-new optimal RWIS network and 2) expansion of current RWIS network. The first analysis was to evaluate the location quality of the current RWIS network in relation to the optimal solution obtained from our model using the two location criteria (i.e., weather and traffic). Since relocating the entire set of existing stations may not be a feasible option, the second analysis was undertaken to suggest a few hypothetical expansion plans over the current RWIS network.

Evaluation of the leveraging effect of existing RWIS stations in neighboring regions

The effect of neighboring RWIS stations for RWIS network planning was evaluated by comparing the coverage of existing RWIS network and all-new equal number of RWIS stations generated by considering available RWIS stations of neighboring states. This is considered essential particularly for developing a statewide RWIS implementation plan, where the primary goal is to leverage all available assets and existing infrastructure in a way that minimizes expending unnecessary resources to further reduce the cost of implementation. Furthermore, by making use of "extra" information available at neighboring sites (i.e., different jurisdictions), nowcasting and forecasting capabilities of an RWIS network will likely be enhanced when compared to that of using information available only at in-state RWIS stations. The results indicated that the deployment of RWIS should take the RWIS of bordering states into consideration.

RWIS Density Guidelines and Their State-wide Applications

The spatiotemporal semivariogram analysis results were used as inputs for RWIS density optimization in order to develop RWIS sitting guideline. RWIS density per unit area for different topographic and weather severity regions were determined from the density optimization outputs. Lastly, density optimization results were used to generate a RWIS density chart for TPI-WSI zones. The RWIS density chart includes upper bound, lower bound and average number of RWIS stations needed for a defined unit area. Using the density chart, RWIS density was determined for fourteen states. The study area is made up of a total of nine different TPI-WSI zones.

Development of a Web-based Visualization Tool

At the end, the developed solutions were integrated into LORWIS (www.lorwis.com) – a prototype web-based RWIS location visualization platform for demonstrating the proposed models and the resulting solutions.

LIST OF ACRONYMS

AADT	Annual Average Daily Traffic
AVHRR	Advanced Very High Resolution Radiometer
BPSO	Binary Particle Swarm Optimization
CDF	Cumulative Distribution Function
DEM	Digital Elevation Model
DOT	Department of Transportation
ESS	Environmental Sensor Stations
FAA	Federal Aviation Administration
FHWA	Federal Highway Administration
GAM	Generalized Additive Model
ITS	Intelligent Transportation Systems
KED	Kriging with External Drift
MODIS	Moderate-resolution Imaging Spectroradiometer
MSE	Mean Standardized Errors
MST	Mean Surface Temperature
NAM	North American Model
NDVI	Normalized Difference Vegetation Index
NIP	Nonlinear Integer Programming
NOMADS	National Operational Model Archive & Distribution System
NWS	National Weather Service
OK	Ordinary Kriging
PSO	Particle Swarm Optimization
RK	Regression Kriging
RMSE	Root Mean Square Error
RSC	Road Surface Condition
RST	Road Surface Temperature
RWIS	Road Weather Information System
SGS	Sequential Gaussian Simulation
SI	Spatial Inference
SK	Simple Kriging
SNODAS	Snow Data Assimilation System
SSA	Spatial Simulated Annealing
TMMS	Traffic Monitoring Management System
TPI	Topographic Position Index
UK	Universal Kriging
VST	Variability of Surface Temperature
WRM	Winter Road Maintenance
WSI	Winter Severity Index

1. INTRODUCTION

1.1 Background

Intelligent Transportation Systems (ITS) is an important part of modern transportation engineering and has a significant impact on society and our everyday life. Its main contribution is to the improvement of transportation mobility and safety, particularly in how it relates to the prevention of weather-related road crashes, a vital and challenging issue, especially for countries with cold regions. In the US, over 1.5 million road crashes, 800,000 injuries and 7,000 fatalities occur annually in the entire United States due to adverse weather (Jin et al. 2014). In Canada, about 3,000 fatalities result from weather-related accidents, and over one in 135 people experience driving-related injuries annually (Andrey et al. 2001). A Road Weather Information System (RWIS) consists of a set of weather and road condition sensors installed at a station near road side. This combination of advanced sensors gathers, processes, and disseminates the road weather and condition information that is then used by road maintenance authorities to make operative decisions before and/or during inclement weather events in order to enhance overall road safety and decrease weather-related crashes. It is also used by travelers via RWIS connected dynamic message signs to help them make more informed decisions when traveling during inclement weather events. But investment in these technologies is significant. Indeed, many North American transportation agencies have invested millions of dollars to deploy RWIS stations to improve the monitoring coverage of winter road surface conditions (White 2006; Kwon and Fu 2017). As transportation authorities are constantly challenged by limited budgets for installing additional stations, it is of paramount importance to address the questions of how many stations are necessary (optimal RWIS density) and where to locate (optimal RWIS location) them to maximize the return on their investment.

There are numerous studies conducted by researchers around the world to quantify the spatial coverage of RWIS data and determine the optimal RWIS density and location based on available RWIS data (Eriksson and Norrman 2001; Manfredi et al. 2008; Kwon and Fu 2013; Kwon and Fu 2017; Kwon et al. 2017). The Federal Highway Administration (FHWA) initiated extensive efforts to provide RWIS sitting guidelines based on the knowledge and experience of field operators

(Manfredi et al. 2008). A more recent study by Kwon and Fu (2017) evaluated the dependency of optimal RWIS density on topographic conditions of the regions under investigation by examining three U.S. states (Iowa, Utah, and Minnesota) and one Canadian province (Ontario). Their findings indicated that more RWIS stations would be needed in mountainous areas than in flatland areas. The study also asserted that a region with a longer spatial autocorrelation range would require fewer stations than a region with a shorter range (Kwon and Fu 2017). In this research we have extended the former work by investigating the dependency of optimal RWIS density on two different measures; namely, topographic and weather severity, in an effort to improve generalization potentials and design a long-term strategic RWIS deployment plan. Since, not only would road surface conditions vary over space but also over time, there is therefore a need to incorporate the temporal domain in the optimization of RWIS location and density.

Spatiotemporal data analysis is a well-known geostatistical analysis technique that is commonly used to analyze the variability of parameters that have a tendency to fluctuate over space and time. It combines spatial and time series analysis concurrently to preserve the interactive effect of time variation on spatial domain and vice-versa. Previous research reveals that spatiotemporal analysis is more accurate than spatial analysis as both time and space are included in spatiotemporal analysis (Graler et al. 2016). The underlying techniques have been previously used to model air pollutants by quantifying the space-time variability of certain particles' concentrations (Graler et al. 2016; Network 2016; Li et al. 2017; Ahmed et al. 2018). Spatiotemporal regression kriging has been used to predict precipitation using Moderate-resolution Imaging Spectroradiometer (MODIS) and Normalized Difference Vegetation Index (NDVI) data (Hu et al. 2017). In a study more relevant to the topic of interest, Wang et al. (2019) investigated spatiotemporal variation of road weather and surface conditions using RWIS data from Alberta, Canada. In this study, the authors developed space-time semivariogram models using RWIS measurements from Alberta in order to examine the applicability of the method. The study's findings provided the spatiotemporal feature of the RWIS database (Wang et al. 2019). However, the dependency of the spatiotemporal feature of RWIS measurements on topographic and weather severity has yet to be scrutinized.

As discussed, there exists a large gap in current literature for determining spatiotemporally optimal density and location of an RWIS network. Equally important, there are no existing guidelines available for winter road maintenance agencies to use and decide its optimality, especially for regions with no RWIS data, which has been deemed a prerequisite for undertaking any RWIS related analyses including location and density.

1.2 Road Weather Information Systems (RWIS)

A Road Weather Information System (RWIS) is a significant part of an Intelligent Transportation System (ITS) infrastructure, especially for countries with regions where winter conditions can significantly affect the mobility and safety of their transportation networks. Information regarding the road surface and weather condition is collected, processed, and distributed by RWIS stations that are generally installed alongside roads and highways. RWIS station consists of atmospheric, pavement and water-level monitoring sensors. The types of data collected by RWIS stations include air, surface, and sub-surface temperatures, precipitation rate, type and intensity, atmospheric pressure, wind speeds and direction, and road surface condition. Major components of an RWIS stations are presented in Figure 1 (Kwon and Fu 2016).
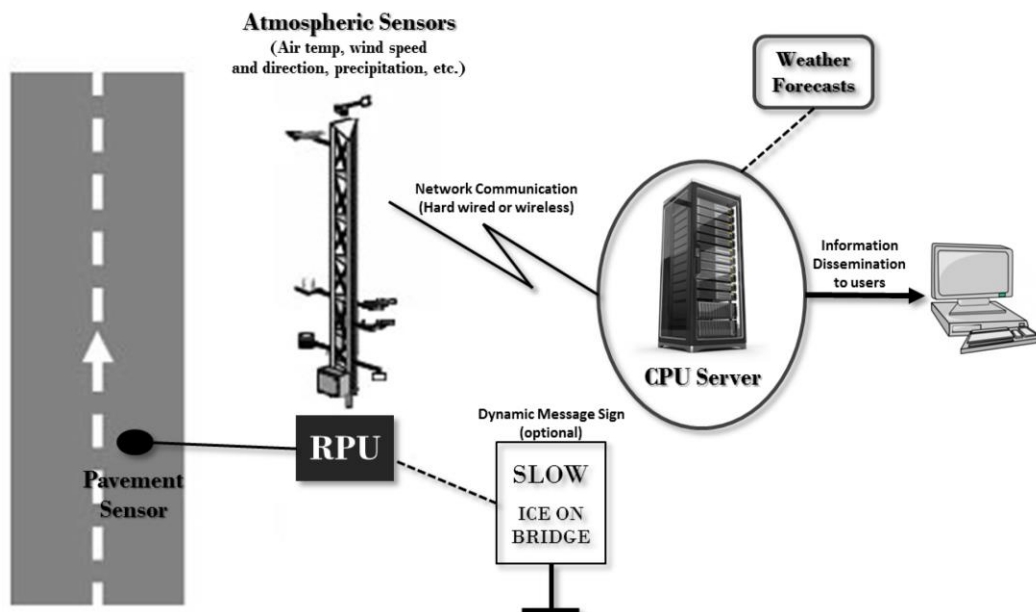
Figure 1: Major components of an RWIS station (Kwon and Fu 2016)

3

Information disseminated by RWIS stations are collectively used by road operations personnel to make effective and timely winter road maintenance decisions, and to help travelers make more informed decisions related to scheduling their trips. The key benefits of RWIS are improved traffic safety, mobility and winter road maintenance (Kwon et al. 2017). Despite these benefits, there are a few limitations associated with both RWIS and the data collected by the stations. The biggest limitation is installation cost, which could be as high as US $100K per station depending on the type and number of sensors (Kwon and Fu 2017). In addition, RWIS data provides point-based measures, which are often limited to capturing the spatial heterogeneity of the surrounding road surface conditions. For this reason, it is important to measure the spatial range of continuity of the measured data and associated variance of the data within the continuity range in order to understand the monitoring coverage of the stations for RWIS network planning issues.

1.3 Current Practice of RWIS Network Planning

The determination for RWIS station sites entails several critical challenges, requiring full understanding and quantification of spatiotemporal variation of road weather conditions and needs for RWIS data. To address these challenges, several studies were conducted to establish proper guidelines for RWIS station installation (e.g., Kwon et al. 2017; Kwon and Fu 2017). An extensive effort was first initiated by the US Federal Highway Administration (FHWA) to provide a standard for RWIS network planning, based on the analysis of published information on siting criteria for weather and pavement sensors, and based on interviews with state's Department of Transportation (DOT) RWIS managers. This study recommended 30 to 50 km (20 to 30 miles) spacing for RWIS station installation based on the knowledge and experience of field operators (Manfredi et al. 2008). Given that the recommended guidelines are based on expert opinion, several researchers attempted to implement a more objective way to quantify the spatial coverage of RWIS data and identify an optimal set of locations and densities of RWIS stations (Eriksson and Norrman 2001; Manfredi et al. 2008; Kwon and Fu 2013; Jin et al. 2014; Kwon et al. 2017; Kwon and Fu 2017).

Several studies were conducted to identify the location and number of RWIS stations required for specific regions. A study was conducted in Sweden to determine the hazardous conditions on a roadway by multiple regression analysis of RWIS data. In this research, ten types of slipperiness

4

were identified to classify road climate and the RWIS site locations were recommended based on the slipperiness (Eriksson and Norrman 2001). Kwon & Fu (2013) presented a GIS-based framework to evaluate RWIS locations in Ontario, Canada, by modelling local road weather conditions (i.e., variability of road surface temperature, mean surface temperature, and snow water equivalent) and topographic location attributes (Kwon and Fu 2013). Jin et al. (2014) proposed an RWIS location optimization method that maximized spatial coverage of existing RWIS sensors based on weather related crash data, which was converted into a safety concern index (Jin et al. 2014). Kwon et al. (2017a) also proposed a new methodological framework, which implemented advanced geostatistical analyses for quantifying the underlying spatial structure of RWIS measurements, and then used an efficient combinatorial optimization algorithm, namely, spatial simulated annealing (SSA) for performing an RWIS network location allocation analysis (Kwon et al. 2017). In their study, the optimization problem was formulated as a nonlinear integer programming (NIP) problem to maximize the monitoring capability, while minimizing kriging errors (Kwon et al. 2017).

Several other studies were conducted in the past with a specific focus on developing an understanding of factors influencing road weather and surface conditions during inclement weather events. Factors influencing road conditions were listed and categorized in a detailed study by White et al. (2006). According to the literature, meteorological, geographical, road construction, and traffic parameters are the factors contributing to the spatial variation in the road surface temperatures (RST). Amongst all the factors, topography was noted as the major factor influencing RST variation over a region (Gustavsson 1990; Boselly et al. 1993; Manfredi et al. 2005; Chapman and Thornes 2005; White et al. 2006). For this reason, Kwon and Fu (2017b) further extended their previous work by examining a hypothesis that the optimal RWIS density or spacing of a region may be dependent on the spatiotemporal variability of road weather conditions as well as their respective topographic settings (Kwon and Fu 2017). To do so, the authors conducted case studies using three US states (Iowa, Utah and Minnesota) and one Canadian province (Ontario). Their results indicated that the number of RWIS stations required would depend on the topographical characteristics of the regions under investigation (i.e., more stations are needed in mountainous regions than in flatter areas). Although their findings have been well received, the study would

benefit from incorporating larger case studies and other variables that can be used to establish a concrete RWIS planning guideline for regions with no RWIS stations.

1.4 Motivation of the Study

The main motivation of this study is to extend our previous work by including more case studies and by further investigating the dependency of optimal RWIS densities on data that are readily available in regions with a need for a long-term strategic RWIS deployment plan. The two measures that we are particularly interested in are Topographic Position Index (TPI) and Winter Severity Index (WSI). TPI is a commonly used topographic measure that defines a relative topographical variation of an area of interest and its neighborhood, whereas WSI is an aggregate indicator of weather severity using yearly average snowfall accumulation and duration, annual duration of blowing snow, and yearly duration of freezing rain (Weiss 2001; Jenness 2006; Mewes 2011). Since both measures are commonly available and believed to influence the number of RWIS stations required, they could be used to develop a new RWIS siting guideline. Furthermore, previous studies dealt solely with spatial domain, which does not account the inherent temporal correlation of road weather and surface conditions. As road surface conditions vary over both space and time, it is necessary to include the temporal domain to achieve more accurate results of RWIS density and location optimization.

1.5 Objectives

Road weather information systems (RWIS) play an important role by helping transportation maintenance operations to keep roadways clear of ice and snow for improved safety and mobility of traveling public. To maximize the benefits of such systems, transportation agencies strive to answer the two key questions: where should we locate RWIS stations and how many do we need in a region with varying environments to provide sufficient coverage over space and time? In this study, we attempt to answer both questions by proposing a new method based on a spatiotemporal geostatistical semivariogram analysis of RWIS data in an effort to determine the topographical and weather characteristics of a region, and how they are related to optimal RWIS densities. In particular, our study will examine the connection between the spatiotemporal autocorrelation range

of RWIS measurements and the topographic and weather characteristics of different zones. The project has the following specific objectives:

- Investigate the topographic and weather characteristics of the study area.

- Investigate spatiotemporal autocorrelation of RWIS measurements (i.e., road surface temperature (RST)) using large scale case studies.

- Examine the effect of topography and weather severity of regions on spatial and temporal continuity of RST data.

- Develop an RWIS optimal density chart that can facilitate the decision-making process for planning a long-term RWIS deployment strategy.

- Evaluate the leveraging effect of existing RWIS stations in neighboring regions

The outcome of this study can be used as a guideline for an RWIS network expansion plan that applies to different topographic and weather severity zones without having to gather any additional data.

2. PROPOSED METHODOLOGY

The topographic and weather characteristics of the study area were analyzed to create several topographically unique regions within the study area with varying levels of winter severity. Spatial semivariogram models were generated for each TPI and WSI class and the change of spatial ranges was evaluated with terrain variability and weather severity classes. Spatiotemporal semivariogram models were then developed to examine spatial and temporal autocorrelation of RWIS data. The effective spatial and temporal range of continuity was determined under different topographic and weather settings, and the dependency of weather data on the topographic variation and weather severity of the region were also evaluated. Then the optimal density of RWIS stations was determined using the modified particle swarm optimization (PSO) method for different topographic and weather classes to develop a TPI-WSI zone based optimal RWIS density chart. Lastly, the density optimization results were used for state-wise application and location allocation under different criteria. An overview of the proposed methodology is presented in Figure 2.
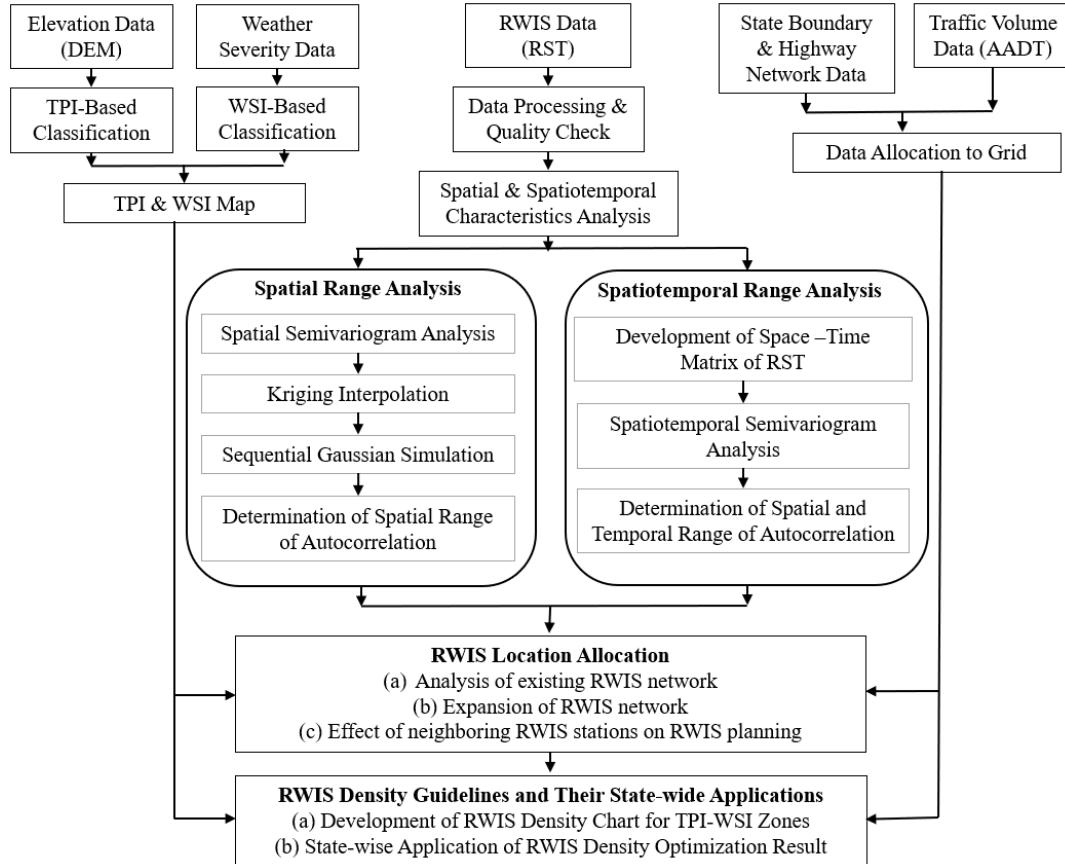
Figure 2: An overview of the proposed methodology

2.1 Characterizations of Topography and Weather

To evaluate the relationship among RWIS station density, topographic variability, and weather characteristics for the regions under investigation, the study area was initially classified into topography and weather-based classes. TPI was calculated using the DEM (Digital Elevation Model) data based on Jenness's algorithm (Jenness 2006). According to the TPI values, the study area was classified into three different landform groups (flatland, hilly, and mountainous). The WSI parameter was used for weather-based classifications using an ESRI shapefile generated for the United States by Meridian Environmental Technology (Mewes 2011). Lower WSI values indicate a less severe weather zone, whereas higher severe weather zones are associated with higher WSI values.

Topography Based Analysis

Topographic analysis was performed using the topographic position index (TPI). TPI values compare the elevation of every point in a digital elevation model (DEM) to the mean elevation of a specified neighborhood around that cell. Hence, the value of TPI defines the topographic variation of a region. Higher TPI values indicate hilly and mountainous areas whereas lower TPI values represent flatlands (Weiss 2001; Jenness 2006). The TPI calculation algorithm was provided by Jenness Enterprises, which is the most promising and widely used algorithm for landform classification (Jenness 2006; Seif 2014a; Mokarram et al. 2015). The equation for TPI for a given location, *i*, is calculated as follows:

$$TPI_i = M_0 - \sum_{n-1} M_n/n \tag{1}$$

Where, M_0 = elevation of the model point, i; M_n = elevation of neighboring points; n = total number of surrounding points employed in the evaluation. Neighborhood is defined as circle or square around the model point. In this study, TPI values for each point were calculated by considering a circular neighborhood with a diameter of 50 km (31.07 mi) around the point. TPI values are sensitive to the neighborhood size and this circle diameter was selected based on the application. For example, a smaller diameter is appropriate for analysis of small landforms such

as individual ridges or valley lines; whereas a larger neighborhood diameter is appropriate for major topographic landforms (Weiss 2001).

Positive TPI values indicate that a point is higher than the average elevation of the neighborhood while negative TPI values represent locations that are lower than the average elevation. TPI values close to zero indicate regions where the elevation is similar to the average elevation of the surroundings (Seif 2014b). Relatively speaking, lower average TPI values indicate flatland, and higher ranges represent hilly and mountainous regions. An illustrated example of TPI values is presented below (Figure 3).

An elevation map of the study area was generated in ArcGIS (ESRI 2015) using Digital Elevation Model (DEM) data. A TPI value was calculated for every 30 m (98.43 ft) grid point (at the resolution of the DEM) using the Topography Tool that follows Jenness's algorithm. Later, the area was classified into three zones based on TPI values.
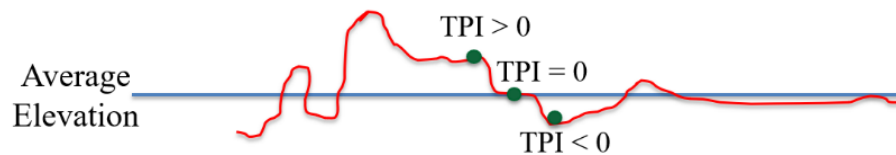
Figure 3: Positive and negative TPI values for a typical land surface

Weather Severity Index

A number of previous studies have introduced methods to calculate WSI, which is generally used as a decision support tool to benchmark the expected amount of road maintenance resources (e.g, salts) are required for a given region in a winter season. A common practice of winter severity investigation is to generate a daily-basis WSI number using some weather parameters and to summarize the numerical values for weekly, monthly, and seasonal WSI (Matthews et al. 2017a and b). There are many different methods currently available to measure winter severity; however, most of the methods are for small geographic area-use only and may not be suitable for use for a large area. A large-scale weather severity mapping method was recently developed by Meridian

Environmental Technology for calculating winter severity over the entire United States and was adopted for use in this study. Parameters used for WSI calculation are yearly average accumulation and duration of snowfall, average annual duration of freezing rain, and blowing snow. Parameters representing weather severity were selected through an iterative process based on previous experiences of the Meridian and the solicitor's interest. Data acquisition details for WSI measurement are listed below:

- Snowfall accumulation data from National Weather Service's United States Climate Normals for the time period of 1971 to 2000 and snow precipitation data from Snow Data Assimilation System (SNODAS) for the winter seasons of 2004 to 2011.

- Snowfall duration data from the METAR observation of weather stations from the Federal Aviation Administration (FAA) and National Weather Service (NWS) for the winter seasons of 2000 to 2010, and analysis of precipitation type from the North American Model (NAM) through the National Operational Model Archive & Distribution System (NOMADS) for the winter season of 2004 to 2011.

- Average annual duration of freezing rain data from METAR observation from 2000 to 2010 winter seasons and analysis of precipitation type from NAM model from 2004 to 2011 winter seasons.

- Hours of blowing or drifting snow was estimated from wind speed data using NAM model through NOMADS and one km AVHRR (Advanced Very High Resolution Radiometer) based land cover data from the University of Maryland for the winter seasons of 2004 to 2011.

The formula used for WSI calculation provides equal weights for all listed factors. As the unit of snowfall accumulation was in inches and annual duration of snowfall, blowing snow and freezing rain, was calculated in hours, the typical 'inches to hours = 10:1' weighting ratio was applied. For extra caution and being proactive, a double weighting factor is provided for the duration of freezing rain. There is no specific explanation for the index values other than it being

a relative comparison of winter severity from a winter maintenance viewpoint (Mewes 2011). The resulting WSI formula is shown below:

Winter Severity = 0.50 × (annual average snowfall in inches) + 0.05 × (annual snowfall duration in hours) + 0.05 × (annual duration of blowing snow in hours) + 0.10 × (annual duration of freezing rain in hours)

The ESRI shapefile generated for United States by the project under Meridian Environmental Technology was used in this research to classify the study area according to WSI.

2.2 Spatial Variogram Modelling

In this study, geostatistical approaches were used for spatial continuity analysis. A semivariogram is a plot of mean semivariance on the *y*-axis versus separation distance between point pairs on the *x*-axis (i.e., lag size). Semivariance is a statistic that measures the similarity between two measurements as a function of separation distance (Olea 2012). Semivariance can be calculated by taking the average of the squared differences between measurements in a spatial domain separated by a specific and defined lag distance, as defined in Equation 2 below:

$$\gamma(h) = \frac{1}{2n(h)} \sum_{i=1}^{n(h)} [z - z(x_i)]^2 \tag{2}$$

Here, $\gamma(h)$ is the semivariance; $z(x_i + h)$ and $z(x_i)$ are two measurements taken at location x_i and $(x_i + h)$, which are separated by a lag with distance, h. Figure 4 shows a typical semivariogram plot.
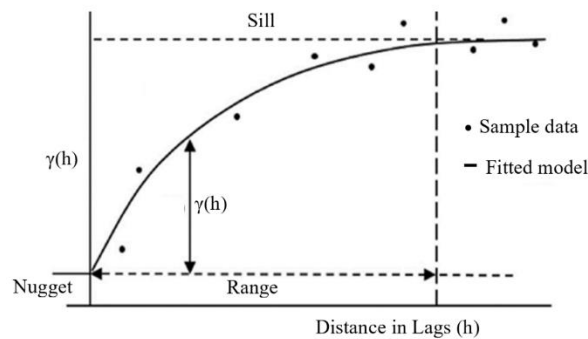
Figure 4: A typical semivariogram with parameters (Kwon et al. 2017)

Three basic parameters are used to define a semivariogram model: range, nugget and sill. The value at the origin (zero separation distance) should theoretically be zero. But due to measurement and sampling errors the value of the semivariogram at the origin could differ significantly from zero, and this error is known as the nugget effect. The semivariance value at which the semivariogram levels off is known as the sill parameter. Generally, a partial sill is the difference between the actual sill value and the nugget effect, which is often the case in a semivariogram analysis. The distance at which the semivariogram reaches the sill value is known as the spatial range of autocorrelation. Autocorrelation is considered as zero beyond this spatial range. Three commonly used semivariogram model forms were considered in this analysis (Bohling 2005; Olea 2006; Solana-Gutiérrez and Merino-de-Miguel 2011). The underlying models are shown in Equation 3 to 5.

$$\text{Spherical model: g(h)} = \begin{cases} c.\left(1.5\left(\frac{h}{a}\right) - 0.5\left(\frac{h}{a}\right)^3\right) & \text{if } h \leq a \\ c & \text{otherwise} \end{cases} \tag{3}$$

$$\text{Gaussian model: g(h)} = c.\left(1 - \exp\left(\frac{-3h^2}{a^2}\right)\right) \tag{4}$$

$$\text{Exponential model: g(h)} = c.\left(1 - exp\left(\frac{-3h}{a}\right)\right) \tag{5}$$

Here, h = lag distance, a = spatial range of continuity and c = sill.

The best-fitting semivariogram models were selected based on their cross-validation results (mean standardized error; correlation between the predictors and observed values; and root-mean-square-error). The semivariogram parameters are used for linear interpolation using kriging, which is a commonly used geostatistical interpolation technique that predicts values at unsampled locations using the weighted averages of surrounding measured observations. Weights are assigned based on the semivariogram model. Commonly used kriging methods are simple kriging (SK), ordinary kriging (OK), and regression or universal kriging (RK or UK). The main difference between simple and ordinary kriging estimation methods is that, SK assumes a constant and known mean over the sampling domain, whereas OK assumes unknown and constant mean. RK and UK are equivalent interpolation techniques that model the trend component of the response variable as a function of either a set of independent predictor variables (as in the deterministic trend

component in RK) or as a function of spatial coordinates (X & Y). The basic equation of kriging is given in Equation 6.

$$Z^*(X_0) = \sum_{i=1}^{n} \lambda_i Z(X_i) \tag{6}$$

where, $Z^*(X_0)$ is the estimated value at location X_0, $Z(X_i)$ is the measured observations at sampling sites X_i, λ_i is the kriging weight and n is the number of sampling location within the search neighborhood. The kriging weight for each sampling location is estimated based on the parameters of the semivariogram model as well as relative distance of the specific point with other sampling points and the unknown point (Lichtenstern 2013; Kwon et al. 2017). However, uneven smoothing is observed in the kriging interpolated surface where smoothing is inversely proportional to data density. This smoothing issue is addressed by geostatistical simulation methods. Sequential Gaussian simulation (SGS) is one of the most commonly used stochastic simulation methods that generates an infinite number of equiprobable realizations using a kriged surface generated from a normal-score-transformed dataset (Olea 2012). Normal-score-transformation (NST) transforms the dataset to a standard normal distribution. The formula for NST for a variable of interest, Z, is given in Equation 7.

$$Y(X_a) = G^{-1}[F^*(Z(X_a))] \tag{7}$$

where, X_a is sampling location with a = 1, 2, 3, …, n; F* is the cumulative distribution function (CDF) of Z and $G^{-1}(.)$ is the inverse Gaussian CDF of the random function $Y(X_a)$. The normal score transformed data is back transformed by applying the inverse of the NST equation. The basic procedure for generating a realization is to define a regularly spaced grid surface of the study area and create a random path through the grids in such a way that, each grid is visited once in each sequence. A simulated value for each grid is generated from the estimated conditional CDF, which is estimated using the kriged surface generated from the available dataset. The simulated value of each grid cell is added to the conditioning dataset for simulating the values of other grid points until all the points in the study area are simulated. For generating the next realization, the same procedure is repeated using a different random path (Chen et al. 2012). In this study, a 5×5 km gridded fishnet of points were generated for each TPI or WSI class and the associated value was

extracted from the SGS surface for each specific class. Finally, a semivariogram was generated using the extracted RST values and the semivariogram range was used for RWIS density optimization.

2.3 Spatiotemporal Semivariogram Modelling

Spatiotemporal semivariogram modeling was used in this study to evaluate the spatiotemporal variability of RWIS measurements. RWIS data for a winter season was downloaded, processed, and a space-time matrix was formulated as an input of the spatiotemporal analysis. The dataset was classified based on previously developed TPI and WSI classes, and a separate analysis was conducted for each month and zone; which were aggregated to generate a seasonal spatiotemporal autocorrelation range for the TPI and WSI classes. Optimal RWIS densities were then determined by relying on spatiotemporal semivariogram analysis results. Density per unit area was calculated and compared for different topographic and weather-based zones.

Geostatistical spatiotemporal semivariogram modeling was used in this study for spatial and temporal continuity analysis. The traditional spatial analysis is incorporated with temporal analysis to consider both spatial and temporal effect. Spatiotemporal analysis is conducted for variables that vary over space and time. A set of variables in a spatiotemporal field can be defined as, $z = \{z(s,t)|s \,\epsilon\, S, t \,\epsilon\, T\}$. Here, S = spatial domain, T = temporal domain. Thus the general equation of a random field, Z is $-z_i = Z(s,t), i = 1,2,3, \ldots \ldots n \times T$. Here, n = number of stations; T = number of time points. The random fields Z (s, t) can be modelled as, $Z(s,t) = \mu\,(s,t) + \varepsilon\,(s,t)$. Here, μ (s, t) = The deterministic part (Trend) and ε (s, t) = The stochastic part (Network 2016). The stochastic part is used for spatiotemporal semivariogram modelling. Spatial and temporal variance is estimated as half of the mean squared difference between pairs of data separated by a user defined spatial (h_s) and temporal lag (h_t) as Equation 8.

$$\gamma(h_s, h_t) = \frac{1}{2n(h_s,h_t)} \sum_{k=1}^{n(h_s,h_t)} [z(s_k, t_k) - z(s_k + h_s, t_k + h_t)]^2 \tag{8}$$

where, γ (h_s,h_t) = estimated semivariance value, n (h_s,h_t) = total number of pairs in analysis domain, $z(s_k,t_k)$ = measurement at spatial location s_k and temporal location t_k (Gething et al. 2007; Shekhar and Zhou 2008). A three-dimensional spatiotemporal semivariogram is presented in Figure 5.

As the estimated model is irregular, a mathematical model was used for smoothening the empirical variogram. The covariance models generally used for spatiotemporal variogram modelling are discussed in the following section.
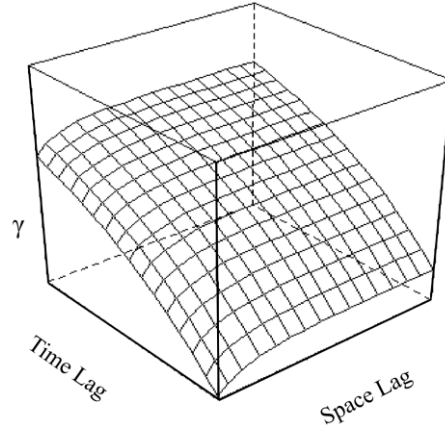
Figure 5: A typical spatiotemporal semivariogram

Covariance Models

A number of covariance models are used for spatiotemporal semivariogram modelling. The most popular and widely used models are described below (Pebesma and Graeler 2012; Graler 2016; Pebesma and Graeler 2019).

Separable Covariance Model
It is assumed in this model that the spatio-temporal covariance function can be represented as the product of a spatial and temporal term. The covariance function can be written as: $C_{sep}(h, u) = C_s(h)C_t(u)$. Thus the equation of variogram is $\gamma_{sep}(h, u) = sill. (\gamma_s(h) + \gamma_t(u) - \gamma_s(h)\gamma_t(u))$. Spatial & temporal sill is ignored in this model and kept constant at 1. A joint sill (= 1) is used; which combines both spatial and temporal effects.

Product-sum Covariance Model

This model assumes a new parameter, k as a weighting factor of the product (k > 0). The equation for the covariance function is $C_{ps}(h, u) = k.C_s(h)C_t(u) + C_s(h) + C_t(u)$. The equation for the variogram can be written as: $\gamma_{ps}(h, u) = (k.sill_t + 1)\gamma_s(h) + (k.sill_s + 1)\gamma_t(u) - k\gamma_s(h)\gamma_t(u)$. The expression of joint sill is $sill_{st} = k.sill_s.sill_t + sill_s + sill_t$. Here, the spatial and temporal nugget is ignored and kept constant at 0; joint nugget is used to account both spatial and temporal effects.

Metric Covariance Model

Identical spatial and temporal covariance functions are assumed in this model, except for spatio-temporal anisotropy. Spatial, temporal, and spatiotemporal distances are treated equally in a joint covariance model by matching space and time by spatiotemporal anisotropy parameter, k (stAni). The equation for the covariance function is $C_m(h, u) = C_{joint}\left(\sqrt{h^2 + (k.u)^2}\right)$. The equation for the metric variogram can be written as: $\gamma_m(h, u) = \gamma_{joint}\left(\sqrt{h^2 + (k.u)^2}\right)$. Temporal distances are internally re-scaled to an equivalent spatial distance to determine the equivalent factor in terms of dependence of 1m separation in a second or a minute. The expression of spatiotemporal anisotropy is $k(StAni) = \dfrac{\text{Spatial unit}}{\text{Temporal unit}} = \dfrac{m}{Sec/min}$.

Sum-metric Covariance Model

This model is a combination of spatial, temporal, and metric models. The equation for a covariance function is $C_{sm}(h, u) = C_s(h) + C_t(u) + C_{joint}\left(\sqrt{h^2 + (k.u)^2}\right)$. The equation for a sum-metric variogram can be written as: $\gamma_{sm}(h, u) = \gamma_s(h) + \gamma_t(u) + \gamma_{joint}\left(\sqrt{h^2 + (k.u)^2}\right)$. Spatial, temporal, and joint nugget are estimated separately in this model.

Simple Sum-metric Covariance Model

This model is the simplified version of the Sum-metric model to restrict the spatial, temporal, and joint variograms to nugget free models. A single spatio-temporal nugget is introduced in this model. The equation for a variogram is $\gamma_{ssm}(h, u) = nug.1_{h>0,u>0} + \gamma_s(h) + \gamma_t(u) + \gamma_{joint}\left(\sqrt{h^2 + (k.u)^2}\right)$. Here spatial, temporal, and joint nuggets are set to 0; Only joint nugget is fitted.

As several previous studies attested the superior performance of sum-metric model in fitting the spatiotemporal variogram using environmental parameters (i.e., smallest mean squared errors), this model was selected and used in this analysis (Hu et al. 2017; Ahmed 2018).

2.4 Location Optimization via SSA

Few research studies have used geostatistical approaches to determine an optimal RWIS density and set of locations. In a study by Kwon et al. (2017), location optimization of RWIS stations was formulated as an integer programming problem, where the objective function was designed to minimize the spatially averaged kriging variance across the road network (Kwon et al. 2017). The problem was formulated on a basic premise that data from individual RWIS in a region should collectively be used to maximize their overall monitoring quality. The method developed, for the first time, provided decision makers with the freedom to simulate and optimize their RWIS network by balancing the needs of the road users, winter road maintenance requirements, and other respective priorities in locating RWIS stations. As such, the underlying idea presented therein has been adopted and implemented in this study.

To improve the generalization potential, spatiotemporal semivariogram parameters generated from different weather and topographic classes were used in the location optimization process as representative of the spatial characteristics of the zones. The highway road network of each state was used as the boundary wherein the solution was limited for location optimization of that specific state. A 5×5 km prediction grid was generated along the road network in ArcGIS to create the candidate sites for RWIS station placement. The objective function was formulated to minimize the mean kriging estimation variance.

The equations of the objective function and its related computation process are shown below.

$$G = \begin{bmatrix} \gamma(x_1, x_1) & \gamma(x_2, x_1) & \ldots & \gamma(x_k, x_1) & 1 \\ \gamma(x_1, x_2) & \gamma(x_2, x_2) & \ldots & \gamma(x_k, x_2) & 1 \\ & & \ldots & & \\ \gamma(x_1, x_k) & \gamma(x_2, x_k) & \ldots & \gamma(x_k, x_k) & 1 \\ 1 & 1 & \ldots & 1 & 0 \end{bmatrix} \tag{9}$$

Where, x_i (i=1, 2, …, k) is the sampling site of a sample subset of size k, and in this case, k is equal to the number of RWIS stations. $\gamma(x_i, x_j)$ is the semivariance between sampling site i and j.

$$g = [\gamma(x_0, x_1)\ \gamma(x_0, x_2)\ …\ \gamma(x_0, x_k)\ 1]' \tag{10}$$

Where, x_0 is the estimation location and x_i (i=1, 2, …, k) is the sampling site of a sample subset of size k. Then the minimum mean square error for ordinary kriging for the estimation location x_0 is:

$$\sigma^2_{OKI}(x_0) = g'G^{-1}g \tag{11}$$

Based on above three equations, the objective function of this work can be formulated as below:

$$f(w) = \frac{\sum_{i=1}^{n-k} \sigma^2_{OKI}(x_0)}{n} \tag{12}$$

where,

$n =$ Total number of candidate RWIS station locations in the study area

Spatial optimization requires mathematical and computational methods to find optimal solutions for an objective function, which is usually performed under some constraints. For the large-size optimization problem, a heuristic algorithm is a suitable and effective method for finding the solutions (Revelle et al. 2008). The optimization method implemented in this study was Spatial Simulated Annealing (SSA) (Kwon et al. 2017), which is a spatial counterpart to simulated annealing (SA) (Kirkpatrick et al. 1983). SSA is a popular heuristic algorithm used to solve spatial optimization problems (Van Groenigen and Stein 1998; Van Groenigen et al. 1999; Heuvelink et al. 2006; Brus and Heuvelink 2007; Kwon et al. 2017). SSA works by slightly perturbing previous sampling designs using random search techniques (Van Groenigen et al. 1999). As optimization continues, it is necessary to avoid local minima, and thus SSA not only accepts improving solutions, but also worsening solutions based on a certain probability (Van Groenigen and Stein 1998). The probability of accepting worsening solutions is typically set initially at 0.2, and this probability decreases exponentially to zero as a function of the number of iterations (Kirkpatrick et al. 1983; Heuvelink et al. 2006; Brus and Heuvelink 2007). The workflow of SSA for a certain number of RWIS stations is displayed in Figure 6.
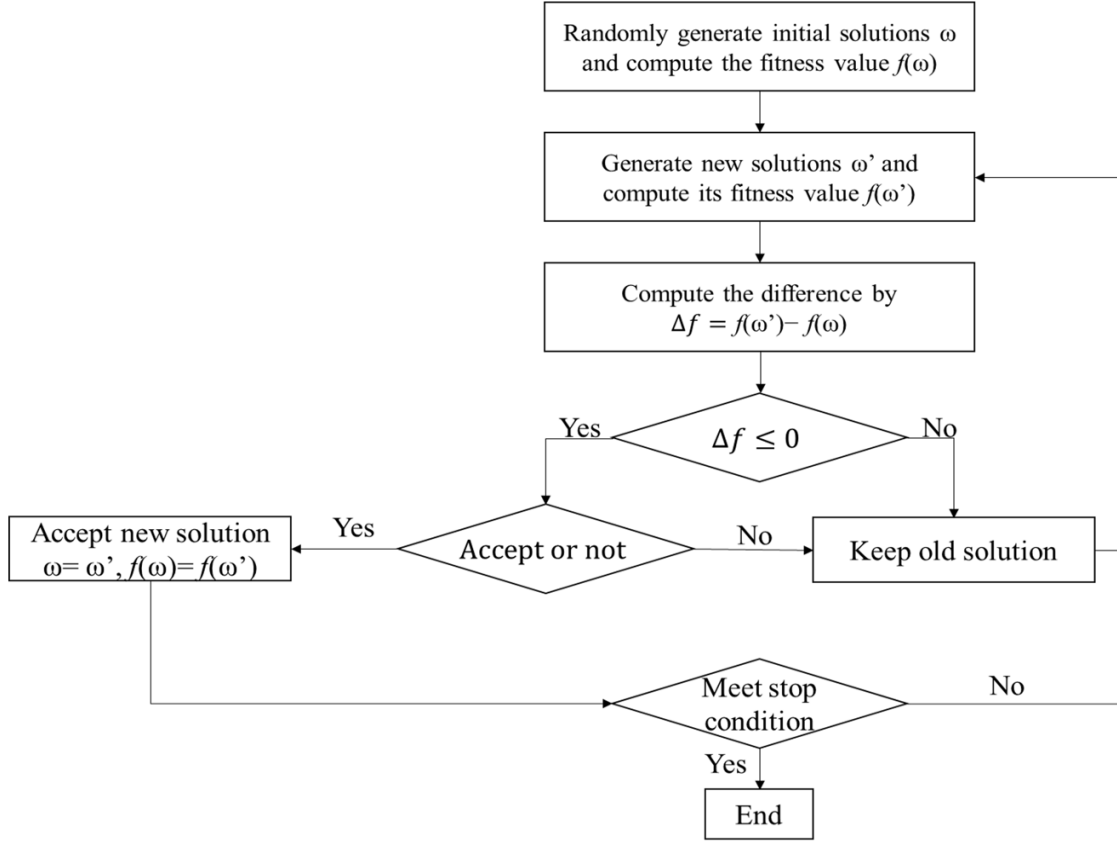
Figure 6: Workflow of Spatial Simulated Annealing (Kwon et al. 2017)

The objective function of this algorithm was the mean OK prediction error variance based on a predefined number of RWIS stations. Optimization follows an iterative process where stations are added one by one into the study area and locations are selected based on heuristic attempts to minimize the objective function. The location optimization was performed assuming an all-new-stations plan for the fourteen States, and an expansion plan that adds 10 and 20 new stations to the existing network. Three different scenarios were used for location optimization: (a) considering weather only, (b) considering traffic only and (c) considering both (both weather and traffic). The Number of iterations was set to 10,000, after which the search process for new RWIS station locations was set to stop. An additional stopping criterion was also used such that if there was no improvement in the objective function after 200 iterations, the algorithm is set to automatically stop. The results of the location optimization are shown in Section 4.4.

2.5 Density Optimization via PSO

Density optimization in this study was conducted in order to compare the number of RWIS stations needed per unit area in different TPI and WSI-based classes. Semivariogram parameters generated from different classes were used in the optimization process as representative of the spatial characteristics of the zones. A randomly selected square region (area of 10,000 square km) within the study area was used as the experimental boundary wherein the solution was limited for density optimization of all classes. Following the same procedure for generating the optimal location solutions, RWIS density curves for different TPI and WSI zones were generated based on a predefined number of RWIS stations. The marginal increment of benefit associated with each additional RWIS stations were calculated to determine the optimal RWIS density.

Density optimization in this project was conducted using Particle Swarm Optimization (PSO). PSO is an evolutionary computation technique and population-based global optimization method developed by Kennedy and Eberhart in 1995 (Shi 2001). PSO is widely used and popular in scientific computations because it is easily implemented and computationally inexpensive. In this optimization process, a number of n-dimensional candidate points (particle) are placed in the search space of a function and each of the particles evaluates the objective function at its current location. Each particle can be assumed as a potential solution presented by velocity and position (Wang 2012; Gu et al. 2019). Movement of each particle is determined based on its best fit location with one or more swarm and the algorithm searches for optima by updating the generations (Kennedy and Eberhart 1995; Poli et al. 2007). The ith particle in the search space can be represented as $x_i = (x_{i1}, x_{i2},\ldots, x_{in})$. Each particle in the swarm flies to the previous best position and global best position; those are named as 'pbest' and 'gbest', respectively. The best previous position of the ith particle can be presented as $p_i = (p_{i1}, p_{i2},\ldots, p_{in})$. The index of the best particle in the swarm is represented by the subscript g. The velocity of particle movement is represented by $v_i = (v_{i1}, v_{i2},\ldots, v_{in})$. The particle is attracted by pbest and gbest during the search process according to Equations 13 and 14.

$$v_{id} = \omega v_{id} + c_1 \zeta (p_{id} - x_{id}) + c_2 \eta (p_{gd} - x_{id}), \qquad (13)$$

$$x_{id} = x_{id} + v_{id}, \qquad (14)$$

where, d = dimension, representing the total number of candidate RWIS sites, where $1 \leq d \leq n$; c_1 and c_2 are positive constant; ζ and η are random adjustment factors with a range of 0 to 1; and ω is the inertia weight. The performance of each particle is measured using a predefined fitness function. A Binary Particle Swarm Optimization (BPSO) was proposed by Kennedy and Eberhart in 1997 for solving integer-programming problems, as the original PSO is not suitable in this case (Kennedy and Eberhart 1997). The basic difference between these two methods is in updating of the particles' position. The sigmoid function is utilized in BPSO where every dimension in the position becomes a number between 0 and 1. A modified BPSO was proposed by Gu et al. (2019) to solve the RWIS location optimization problem (Gu et al. 2019). The similar method was adapted for use in our study for region-wise RWIS density optimization. Position of particle is updated using Equation 15.

$$x_{id} = \frac{1}{1+e^{-v_{id}}},$$ (15)

In the modified BPSO, a threshold probability, r is set to control whether the x_{id} becomes 1 or not; where 1 represents the selection of the element. During optimization the total number of RWIS stations (m) is set as a constant and the algorithm is set to select best-fit 'm' number of locations in the search space. The original BPSO shows premature convergence because of a quick loss of diversity. To treat this problem, more randomness is added into the internal mechanism of the modified BPSO in order to expand the search space and allow the particle to escape from any possible local minima. Another addition is that, if more than one location has the same probability for an RWIS station, a mechanism is set in the modified BPSO to randomly select one of them as the solution. Lastly, in addition to the maximum velocity set to control the speed of convergence, the inertia weight (ω), and self-learning factor (c1) are set to decrease from 0.9 to 0.4 and 2 to 0, respectively, in the search process. On the other hand, the society-learning factor (c2) is set to increase from 0 to 2. The parameters are chosen to ensure that the particles can fly slowly while eliminating their ability for self-learning and enhancing social-learning. The steps associated with the modified BPSO algorithm are listed below (Poli 2007; Wang 2012; Gu et al. 2019).

Step 1. 'm' particles are initialized with dimensions of velocity.

Step 2. Velocities are converted to positions (probabilities) using the Sigmoid function (Equation 8).

Step 3. Two top probabilities are selected in each particle's position and they are set to the selected candidate points for locating RWIS stations, then ordinary kriging variance is calculated for all the unknown points as the fitness value.

Step 4. Memorize the current individual best positions and the global best positions.

Step 5. Update ω, c1 and c2 using Equation 16, 17 and 18.

$$\omega_{new} = \omega_{old} - \frac{\omega_{max} - \omega_{min}}{number\ of\ iterations}, \tag{16}$$

$$c_{1new} = c_{1old} - \frac{c_{1max} - c_{1min}}{number\ of\ iterations}, \tag{17}$$

$$c_{2new} = c_{2old} - \frac{c_{2max} - c_{2min}}{number\ of\ iterations}, \tag{18}$$

Step 6. Update each particle's velocity using Equation 19.

$$v_{id} = \omega v_{id} + c_1 * \zeta_{id} * \Delta x_{pid} + c_2 * \eta_{id} * \Delta x_{gid}, \tag{19}$$

If the $v_{id} > v_{max}$, then $v_{id} = v_{max}$.

Step 7. Update particles' positions using Equation 8.

Step 8. Update the individual best position and global best position by comparing fitness values. If updated fitness value is smaller than before, accept the new solution, check if the new solution meets the stopping criterion (i.e., a predefined number of RWIS). If not, repeat the process from Step 2.

3. STUDY AREA AND DATA DETAILS

3.1 Study Area and RWIS Network

The study area for spatiotemporal analysis and RWIS density optimization was selected based on RWIS data availability and distribution of RWIS stations to cover a variety topography and weather conditions that may pose challenging driving conditions. Eight states had sufficient data, RWIS station coverage, and number of stations for our analysis, including: Colorado (CO), Iowa (IA), Kansas (KS), Kentucky (KY), Minnesota (MN), Nebraska (NE), Ohio (OH) and Wyoming (WY). These eight states provide a broad enough region, as well as a range of topographic and weather conditions, in which to explore our approach. The total available RWIS station count for the states are: CO (147), IA (86), KS (56), KY (38), MN (98), NE (70), OH (182) and WY (81). The study period selected for this project included a winter season (October 2016 to March 2017) to best capture challenging winter driving conditions. Distribution of RWIS stations for the study area is presented in Figure 7.

The spatiotemporal semivariogram analysis results were then applied to RWIS location optimization for fourteen states presented in Figure 8. The total available RWIS station count for the additional states are: California, CA (23); Delaware, DE (19); Illinois, IL (59); Michigan, MI (97); North Dakota, ND (29); Pennsylvania, PA (19); Utah, UT (98); Virginia, VA (52); and Wisconsin, WI (59).
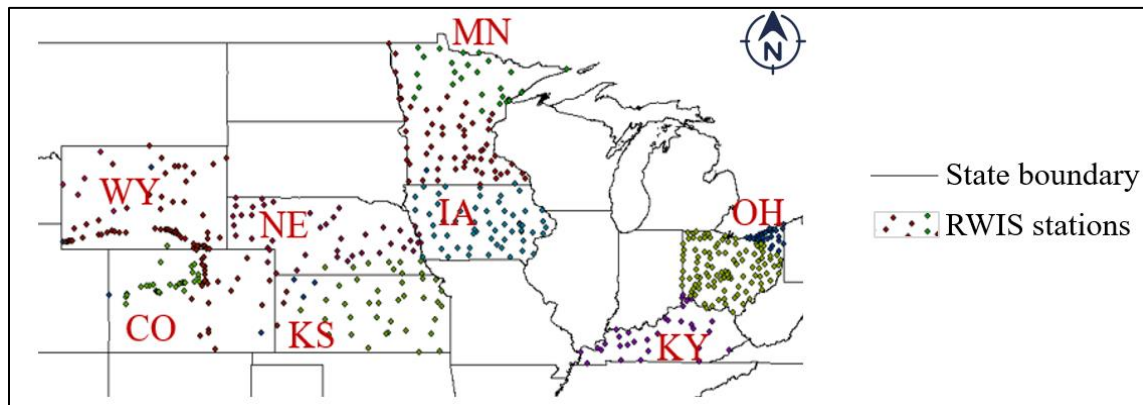
Figure 7: Distribution of RWIS stations for eight US states
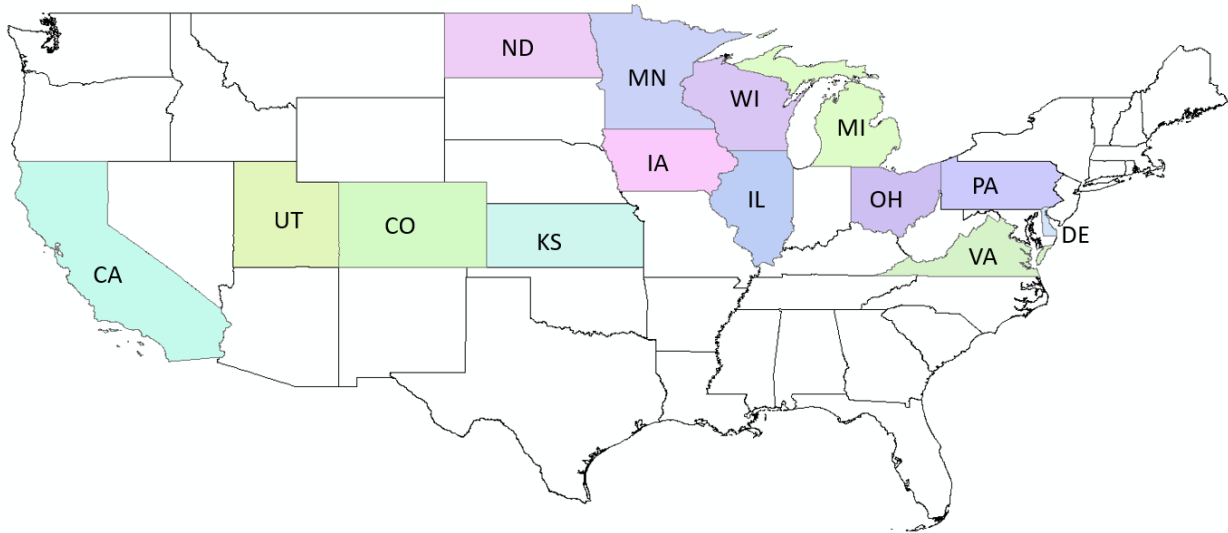
Figure 8: Study area for location optimization

3.2 Data Description

The description of various data sources which are used in this study are described in this section.

Topography Data

Digital Elevation Model (DEM) with resolution of 30 m data (28 GB) was downloaded from USGS website (https://earthexplorer.usgs.gov/) for topographic characteristic analysis in ArcGIS 10.4.1 for twenty US DOTs. The resulting TPI map file has a size of 49 GB.

Weather Severity Data

The ESRI shapefile generated by Meridian Environmental Technology was used for weather severity analysis.

RWIS Data

RWIS data was downloaded from Iowa State University (http://mesonet.agron.iastate.edu/RWIS/) and collected from state DOTs. The state-wide RWIS data was downloaded as an excel file. Measurements from a typical RWIS station includes, but not limited to, air and surface

25

temperature, visibility, wind speed and road surface conditions, collected at 15 to 20-minute interval. In total 1026 stations are included in the analysis and 4368 hours of data was used.

Traffic Volume Data

Annual average daily traffic (AADT) data for the year 2017 was downloaded from TMMS (Traffic Monitoring Management System) section of Ohio Department of Transportation website (http://www.dot.state.oh.us/Divisions/Planning/TechServ/Pages/default.aspx). AADT data includes location description, details of route, AADT and some other information. Size of AADT data covering 8760 hours of observations is 2.22 GB.

3.3 Data Processing

RWIS data were processed to remove the missing and erroneous data using five steps: (a) Data completeness test to identify missing data, (b) Reasonable range test to find erroneous data, (c) Cross-checking RST data with air-temperature data, (d) RST data pattern analysis and (e) Detrending RST data with respect to time using Generalized Additive Model (GAM).

Data completeness was checked by identifying the total missing data for each sensor. If the total missing data is more than 15%, the associated sensor ID was marked and the data from that sensor was not used for analysis. Reasonable range was tested based on historical data ranges for the associated region and month. Filtered RST data were then cross-checked with air-temperature data ranges for any possible outliers. An RST data pattern analysis was performed by plotting the day of the month versus the average daily temperature for all selected sensors, for each state, and each month. All selected sensors were expected to show a similar pattern throughout the month. If any unusual pattern was noticed the RST data for the associated sensors were further investigated for the time period of the unusual pattern. In total, 48 sets of data (six months for eight states) were analyzed using the above described process. Finally, RST data was de-trended with respect to time using a Generalized Additive Model (GAM); where GAM worked as a generalized linear model with linear predictors. The GAM function was formulated as: $m = \beta_0 + f_1(x_1) + f_2(x_2) + \cdots + f_i(x_i)$. Here, m = variable of interest, β_0 = intercept, $f_i(x_i)$ = smooth function of predictor x_i. the

smooth function can be expressed as: $f_i(x_i) = \sum_{n=1}^{m} s(x_n)$ (Hastie and Tibshirani 1990; Wang et al. 2019).

Descriptive statistics (means and standard deviations) revealed relatively less variation in average monthly temperatures in the mid-winter months than in the shoulder months. Overall minimum and maximum temperatures for the study area were: -30.3˚C to 51.5˚C (-22.5˚F to 124.7˚F). Table 1 presents the maximum, minimum, average, and standard deviations of RST for the study area. Because of erroneous data in November 2016 in Kentucky, it was excluded from the analysis. Figure 9 shows the seasonal maximum, minimum, average and standard deviation of RST for the study area.

Table 1: Descriptive Statistics of RST for the Study Area (Winter Months of 2016-17)

States		CO	IA	KS	MN	OH	KY	NE	WY
Oct-16	Min	-6.7	-1.1	0.8	-2.6	-1.5	-7.2	-6.2	-9.4
	Average	15.5	16.9	20.8	12.6	18.3	20.0	16.7	11.9
	Max	37.8	41.5	46.2	41.0	47.0	39.5	44.7	45.1
	StDev	9.0	6.9	8.2	7.0	6.9	6.9	7.7	8.1
Nov-16	Min	-29.8	-8.6	-7.6	-9.9	-24.0	-	-12.5	-15.9
	Average	7.6	9.5	12.5	6.0	10.1	-	8.7	5.0
	Max	46.9	38.3	39.5	30.2	35.5	-	34.4	30.6
	StDev	9.2	7.1	7.8	6.2	6.3	-	8.0	8.0
Dec-16	Min	-22.6	-29.5	-24.9	-29.9	-19.6	-10.4	-28.1	-29.5
	Average	-1.5	-2.7	0.8	-6.6	1.7	4.5	-3.3	-5.4
	Max	26.6	18.8	22.9	11.7	51.5	21.1	17.8	17.6
	StDev	7.4	6.4	7.3	6.8	5.7	4.8	6.2	6.3
Jan-17	Min	-26.9	-24.0	-20.9	-30.3	-19.1	-17.2	-26.9	-29.1
	Average	-0.6	-2.1	2.7	-6.8	2.9	6.4	-2.5	-5.5
	Max	37.8	19.6	28.5	14.2	25.5	21.8	19.9	21.0
	StDev	7.7	6.0	7.4	7.9	6.3	5.1	6.3	6.9
	Min	-17.7	-15.9	-10.8	-26.0	-22.7	-9.6	-19.4	-23.4

Feb-17	**Average**	6.0	5.6	9.8	-1.5	7.1	9.3	4.4	0.9
	Max	37.7	32.4	38.6	27.2	34.5	30.4	36.1	30.7
	StDev	8.9	8.2	9.0	8.1	7.3	5.9	8.0	7.7
Mar-17	**Min**	-17.2	-16.4	-7.3	-22.0	-10.8	-8.4	-11.5	-17.5
	Average	11.0	7.0	13.9	2.5	9.0	12.1	9.4	7.2
	Max	38.3	36.1	48.7	36.3	36.0	31.7	43.7	39.5
	StDev	10.2	7.6	9.5	8.7	7.1	6.5	8.3	9.3
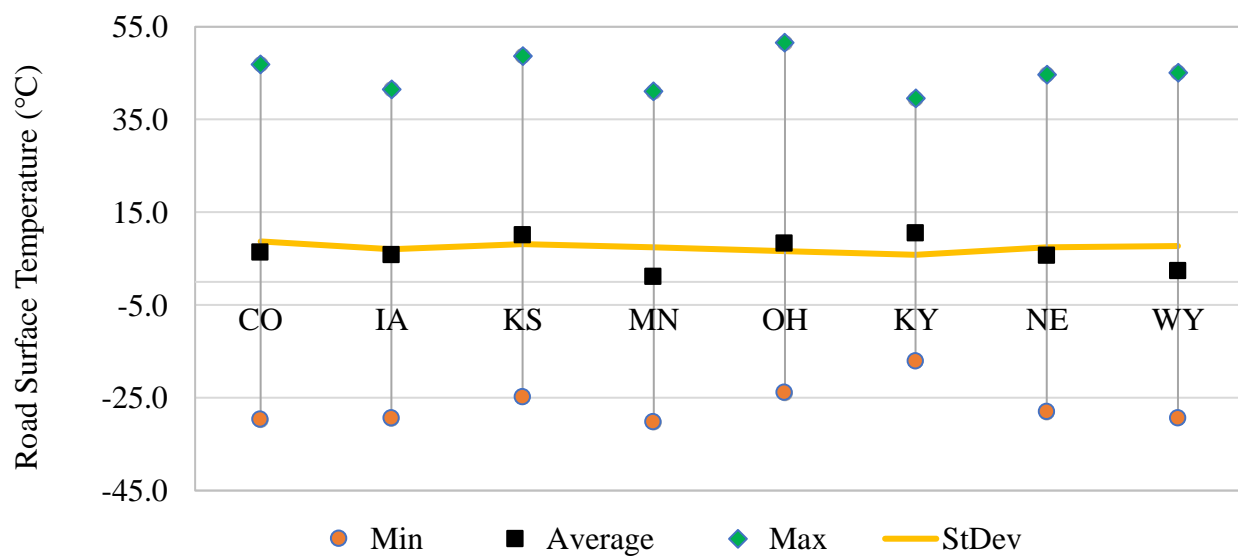
Figure 9: Seasonal road surface temperature details for eight states

Semivariogram modeling and RWIS location optimization were performed using the R statistical package - version 3.2.5 (Pebesma 2004; Graler et al. 2016; R Core Team 2018). RWIS density optimization was coded in Python. To improve the computational efficiency, all optimizations undertaken in this study were run on the supercomputer "beluga" from the "University of Alberta", managed by Calcul Québec and Compute Canada (https://www.computecanada.ca/); with 32 CPUs, each of which runs on 2.4 GHz CPU and 1GB memory.

4. RESULT AND DISCUSSION

4.1 TPI and WSI Classes

Topographic features of the twenty US states were studied, quantitatively described, and classified using the topographic position index (TPI). The TPI map of our study area is shown in Figure 10, and the range of values was between – 565 and 5293. As our main interest in using TPI-based analysis was landform classification over a large extent, the absolute value of TPI was used. However, much of our study area had a TPI value below 75. More specifically, IA, MN, ND, WI, IL, MI, IN (Indiana), OH, KY, VA, PA, NY, DE and a large portion of NE, KS and CA had TPI values that were less than 75. This area was designated as TPI class 1 (i.e., the light coral colored zone in Figure 10), that represents the flatland area. Few points with a TPI value between 75 and 1500 can be seen at the edges of VA, PA, NY and CA. Another large part of the study area had a TPI range between 1900 and 2100 with a minor area of 1500 to 1900. This zone (TPI 2 – hilly area, gray colored zone in Figure 10) covers a small part of KS and a sizable portion of NE, CO and WY; and a very small part of UT and CA. Large variations in TPI can be seen in the remaining study area, including a large part of CO, WY, UT, NV (Nevada) and CA where the range in TPI varied from 1900 to 5293 with a minor area under 1900. This zone was classified as TPI class 3 – mountainous region.
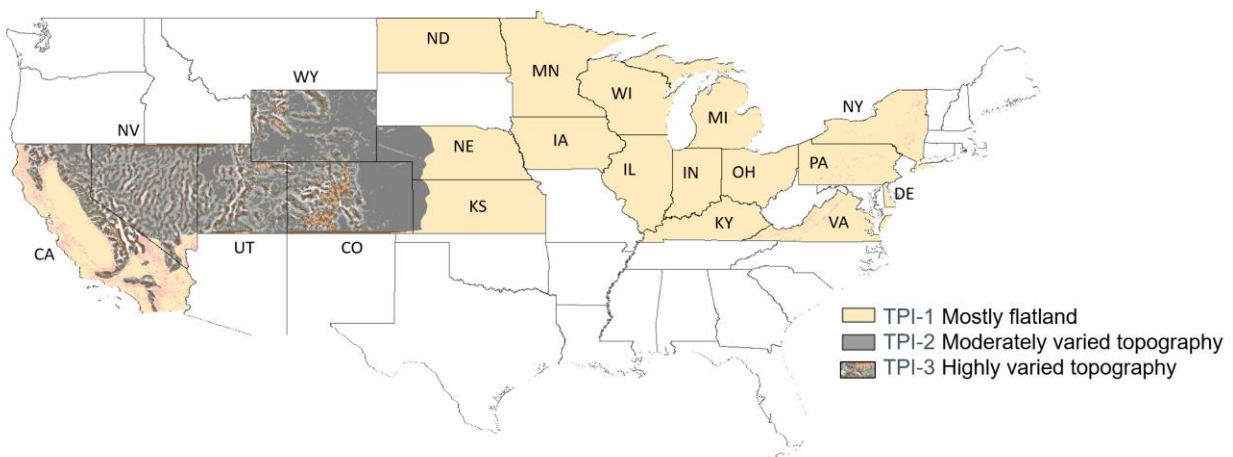
Figure 10: TPI map of the twenty US states

The study area was also classified into four WSI classes (Figure 11). The range of WSI was 7.6 to 301.7. Class – WSI 1 (blue coloured zones) includes a zone with WSI values less than 25. This area nearly covers all of KY, KS, VA and DE; lower part of IL and IN; a small part of PA, CO, UT, NV and CA states. The second class – WSI 2 (green colored zones) represents a region with a WSI range of 25 to 50. OH, IA, NE; southern half of MN, ND, WI; Northern part of IL, IN and a small portion of PA, NY, CO, WY, NV are captured by this class. From the remaining portion of the study area, a relatively large region is between 50 to 75 WSI and 75 to 100 WSI. The region (50 to 100) was included in class – WSI 3, and this class covered the northern part of MN, ND, WI, PA, NY a small portion of OH and CO, and part of WY. The remaining area had a large variation in WSI values from 100 to 301.7. This area is mountainous and was classified into WSI class 4, which is quite similar to class – TPI 3.
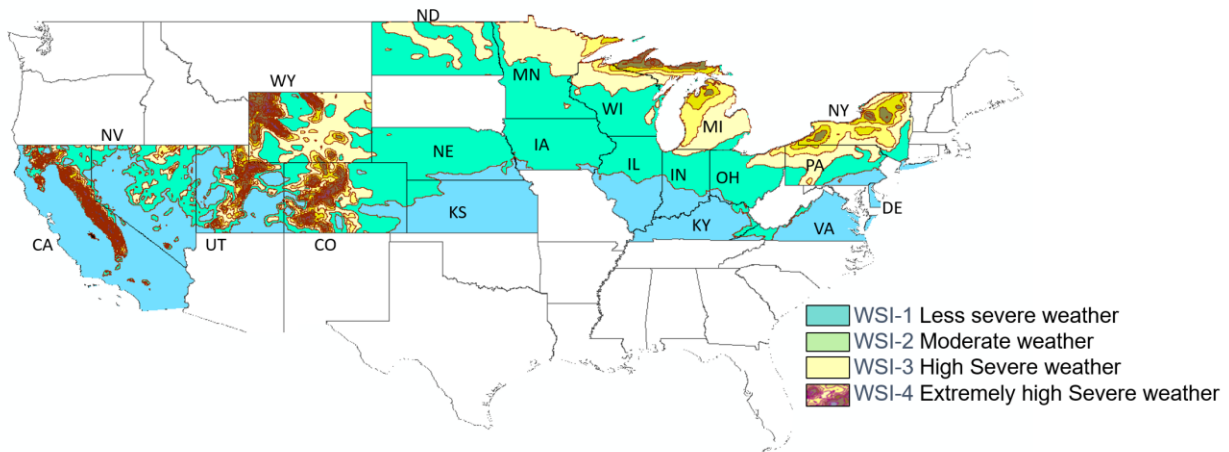
Figure 11: WSI map of the twenty US states

4.2 Spatial Semivariogram Modeling Results

The range of spatial autocorrelation for the study area was examined using semivariogram analysis. RST has been selected as the variable of interest for this study as it is one of the most widely used weather variable that represents the road surface conditions properly as well as a necessity for improved winter road maintenance operations (Kwon and Fu 2017). Raw RST data were processed and semivariogram models were developed using monthly average RST data.

The range of spatial autocorrelation for three of the TPI-based classes and four of the WSI-based classes are presented in Figure 12 . We can see that for TPI class 1 - the flatland area - the average spatial range is the highest, followed by TPI 2, and TPI 3, suggesting that on average the range of spatial structure (i.e., similarity in conditions) decreases as topography becomes more variable. Similarly, decreasing spatial range is observed from WSI 1 to WSI 4. Given the limited time periods examined here, a lack of data, and clustering of RWIS stations when multiple states were considered together, monthly estimates for spatial ranges (colored bars) do not always follow the average trend. Besides, the spatial range for WSI 1 for the month January is missing because the semivariogram developed for this particular month failed to converge, possibly due to a lack of samples to capture the underlying spatial autocorrelation structure of the variable of interest. This result reveals that the predictive coverage of a RWIS station is dependent on the topographic and weather features of a region. Flatter areas had higher spatial ranges and thus require a smaller number of RWIS stations to achieve a similar level of monitoring coverage than hilly or mountainous regions. Correspondingly, areas with more severe weather conditions require more stations to achieve the same level of spatial coverage than areas with less severe weather. This phenomenon is examined using density optimization in the following section of this paper.
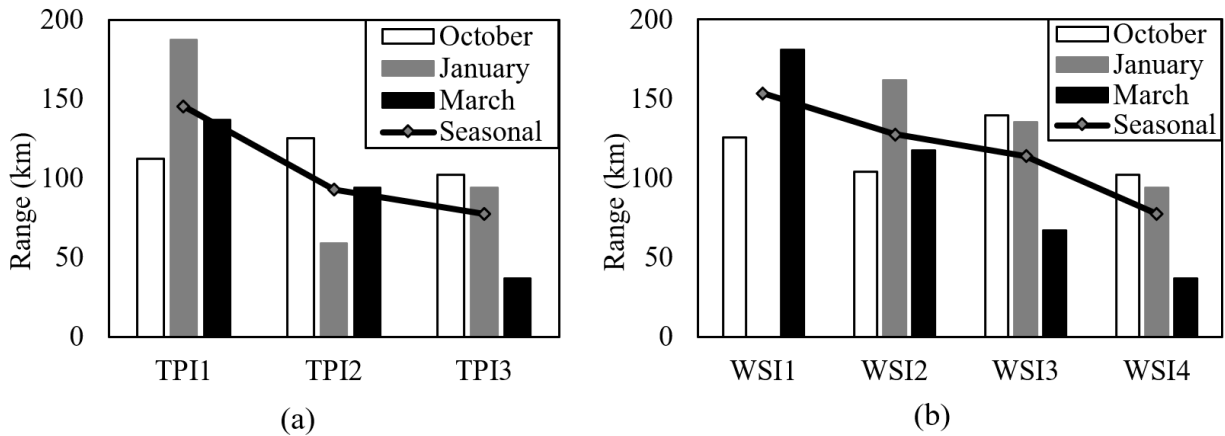
Figure 12: Comparison of spatial range for (a) TPI – based classes (b) WSI – based classes.

4.3 Spatiotemporal Semivariogram Modeling Results

RWIS data for the study area were also processed considering both space and time domains on a monthly basis, from October 2016 to March 2017. Road surface temperature (RST) data were aggregated using twenty- minute interval for time domain analysis. Space-time matrix was then

formulated for each TPI and WSI zones. Spatiotemporal autocorrelation of RST for each study zone was then analyzed using spatiotemporal variogram modelling methods using gstat package in R (Pebesma 2004; R Core Team 2018). A sample of spatiotemporal semivariograms of different TPI and WSI classes is presented in Figure 13. Seasonal spatiotemporal analysis results for TPI and WSI zones are presented in Figure 14.
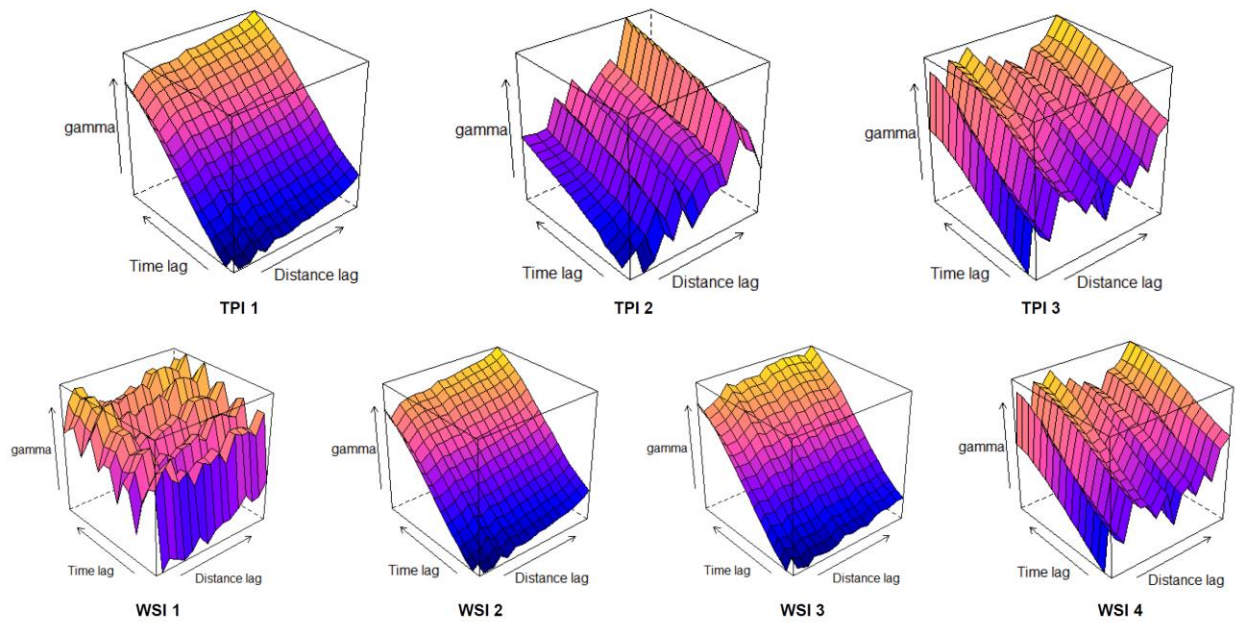
Figure 13: A sample of spatiotemporal semivariogram of TPI and WSI classes for RWIS data of November 2016
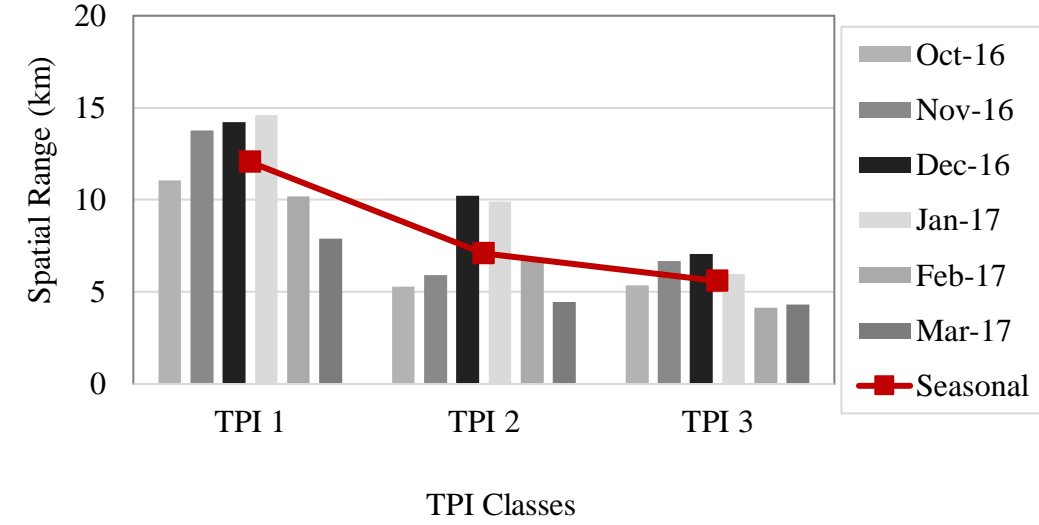
(a)
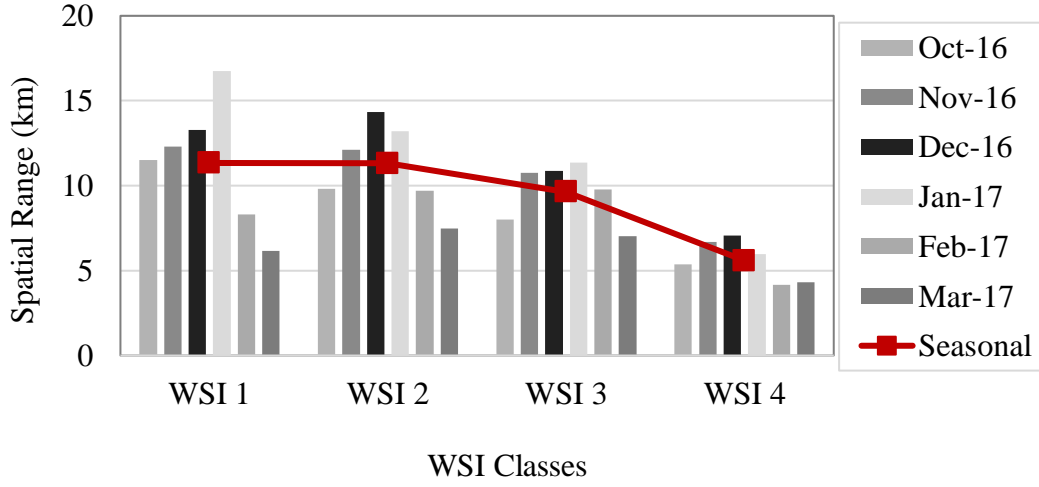
(b)

Figure 14: Spatial semivariogram ranges for (a) TPI class and (b) WSI classes

According to Figure 14, relatively higher spatial and temporal ranges are obtained for TPI class 1 (flatland area); followed by class 2 and 3 representing hilly and mountainous areas, respectively. Similar results were obtained for weather-based classes, where regions with less topographic variation and less severe weather have a higher spatial and temporal range as depicted in Figure 15. The range of autocorrelation decreases with the increase of topographic variation and weather severity. In general, there is a trend of higher autocorrelation range during mid-winter months compared to shoulder months, which is as expected.
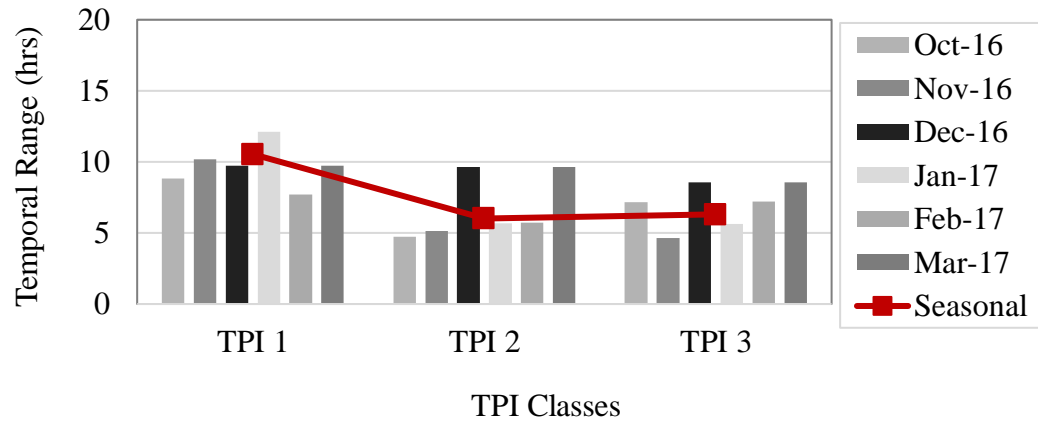
(a)
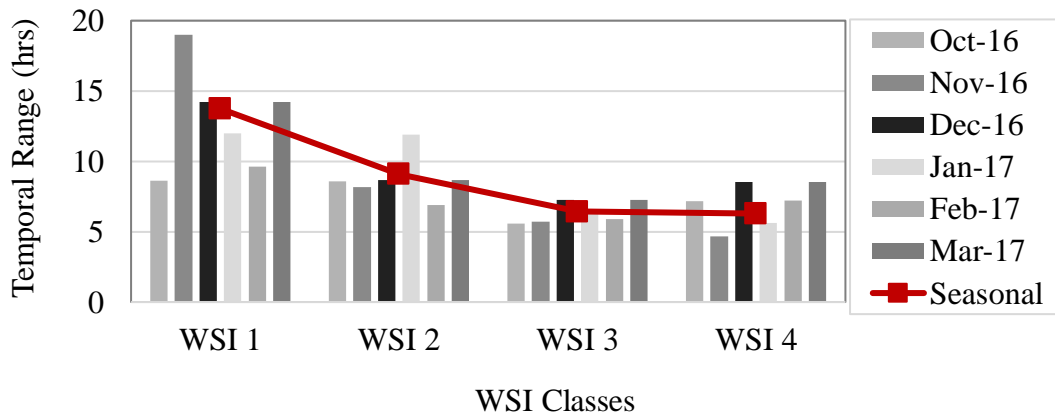
(b)

Figure 15: Temporal semivariogram ranges for (a) TPI class and (b) WSI classes

The effect of weather severity in the TPI 1 zone, which is the flatland area, is presented in Figure 16. In our study area, the flatland region consists of three weather severity regions and there is a trend for higher autocorrelation range in areas with less weather severity than areas with more severe weather severity regions, especially for the temporal range. The effect of weather for the spatial range is negligible as the total difference is only 1.6 km. From this, we can conclude that topography can serve as a more intuitive measure for RWIS network planning than that of weather severity. Similar comparisons for other TPI zones have not been made because TPI 2 zone consists of WSI 2 and 3 zones; and TPI 3 zone is identical to WSI 4 zone (see Figure 10 and Figure 11).
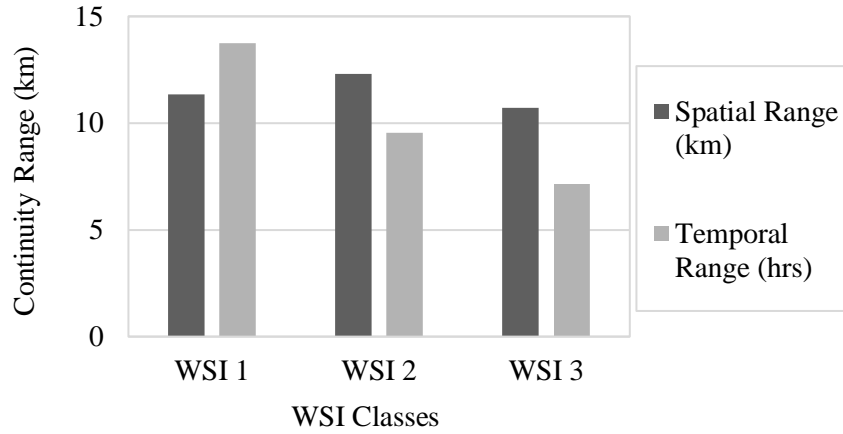
Figure 16: Spatial and temporal range for flatland area (TPI 1) with different weather severity

4.4 State-wide RWIS Implementation Strategies

Spatiotemporal semivariogram models for different topographic and weather severity regions were used for state-wise RWIS network implementation. This section includes the state-wise relocation of current RWIS network for different criteria, state-wide expansion of the RWIS network, and the effect of spatial demarcation in RWIS network planning.

A State-wide Relocation of the Current RWIS Network

This section conducts an analysis of the hypothetical problem of optimizing RWIS network for each state such that the current network can be effectively evaluated. The main goal of this state-wise relocation is to compare the overall monitoring capabilities of the optimized network with the current location settings. The existing station number was collected from Iowa State University website and the equal number of all-new RWIS station locations were generated for candidate states using a dual scenario; that is considering both weather and traffic data with equal weightage. The resulting locations for all-new RWIS stations are presented in Figure 17 and the location information is provided in Appendix A.

CA

CO

DE

IA

KS

IL
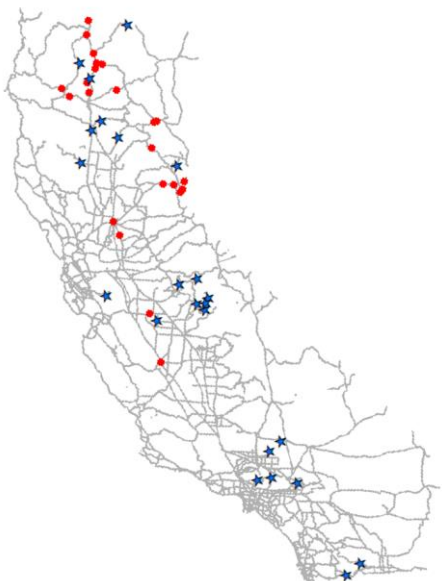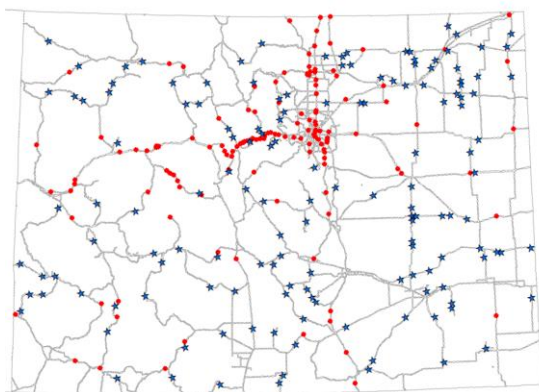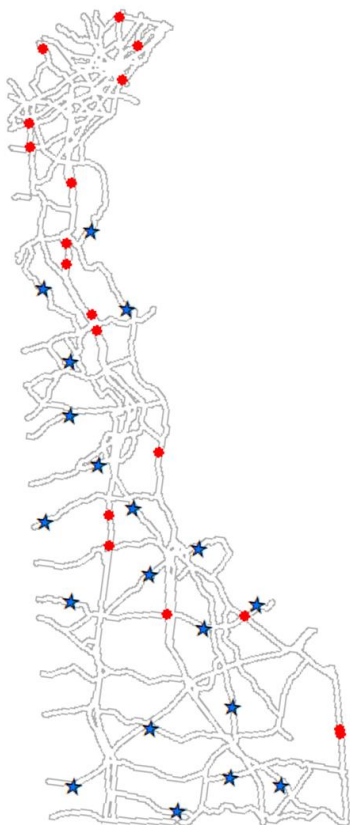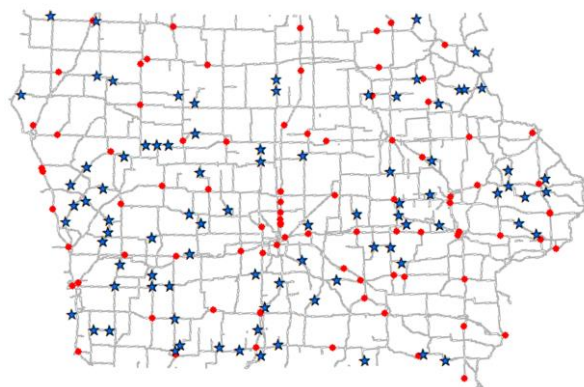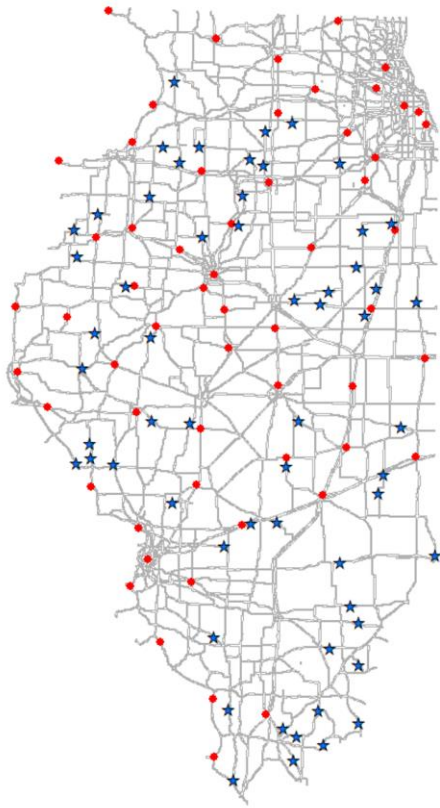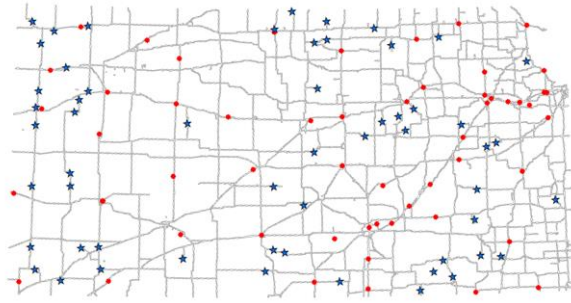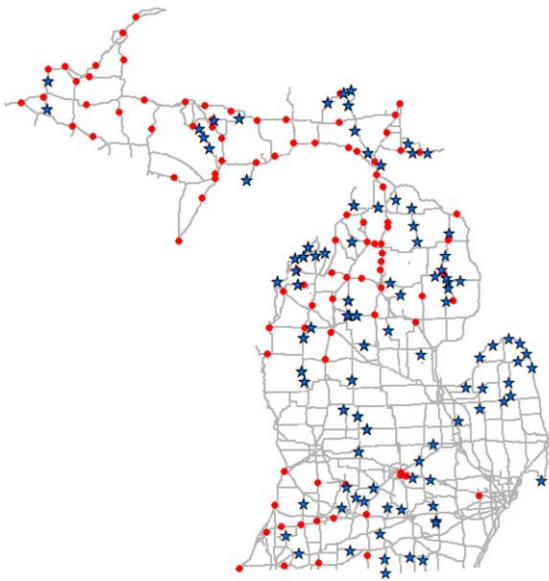
MI
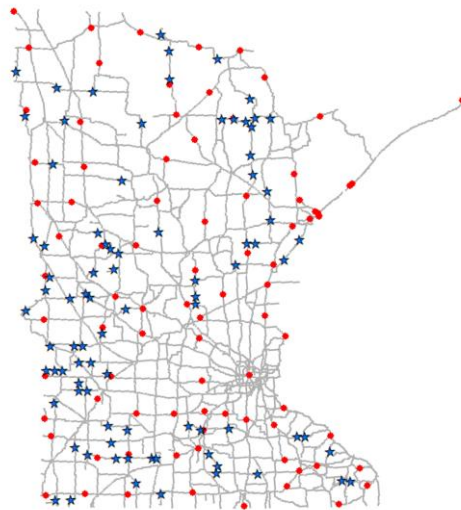
MN
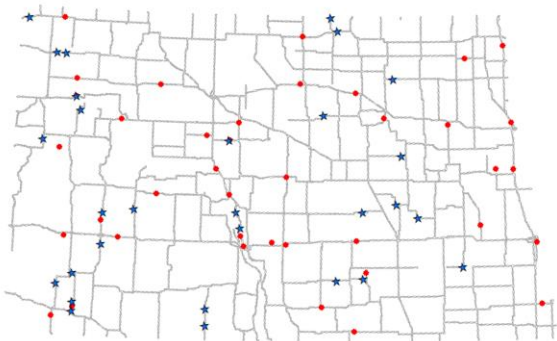
ND
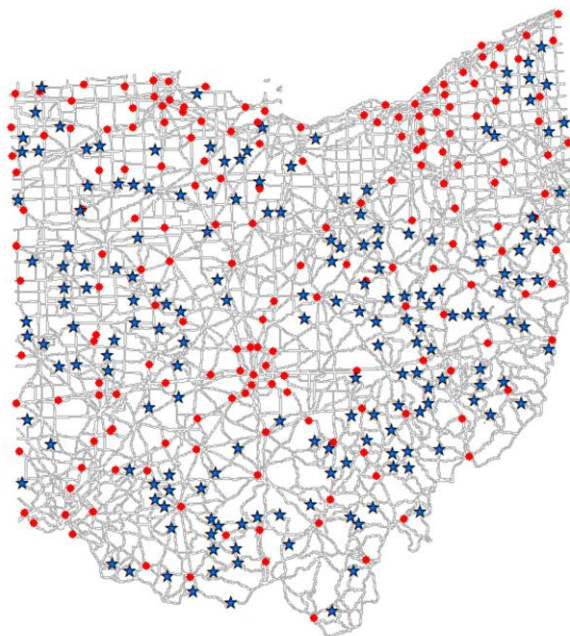
OH
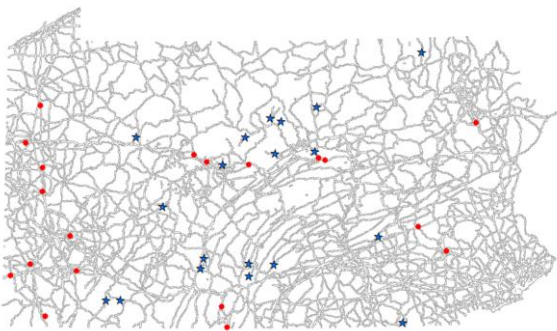
PA
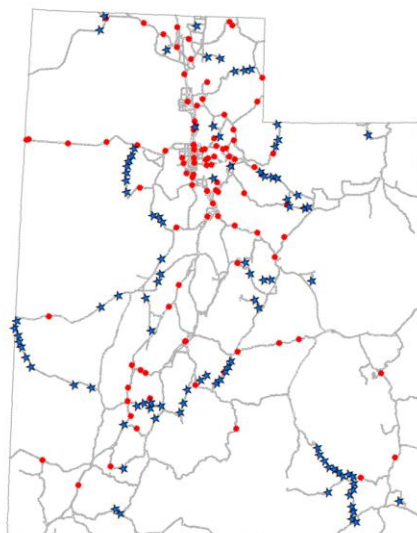
UT
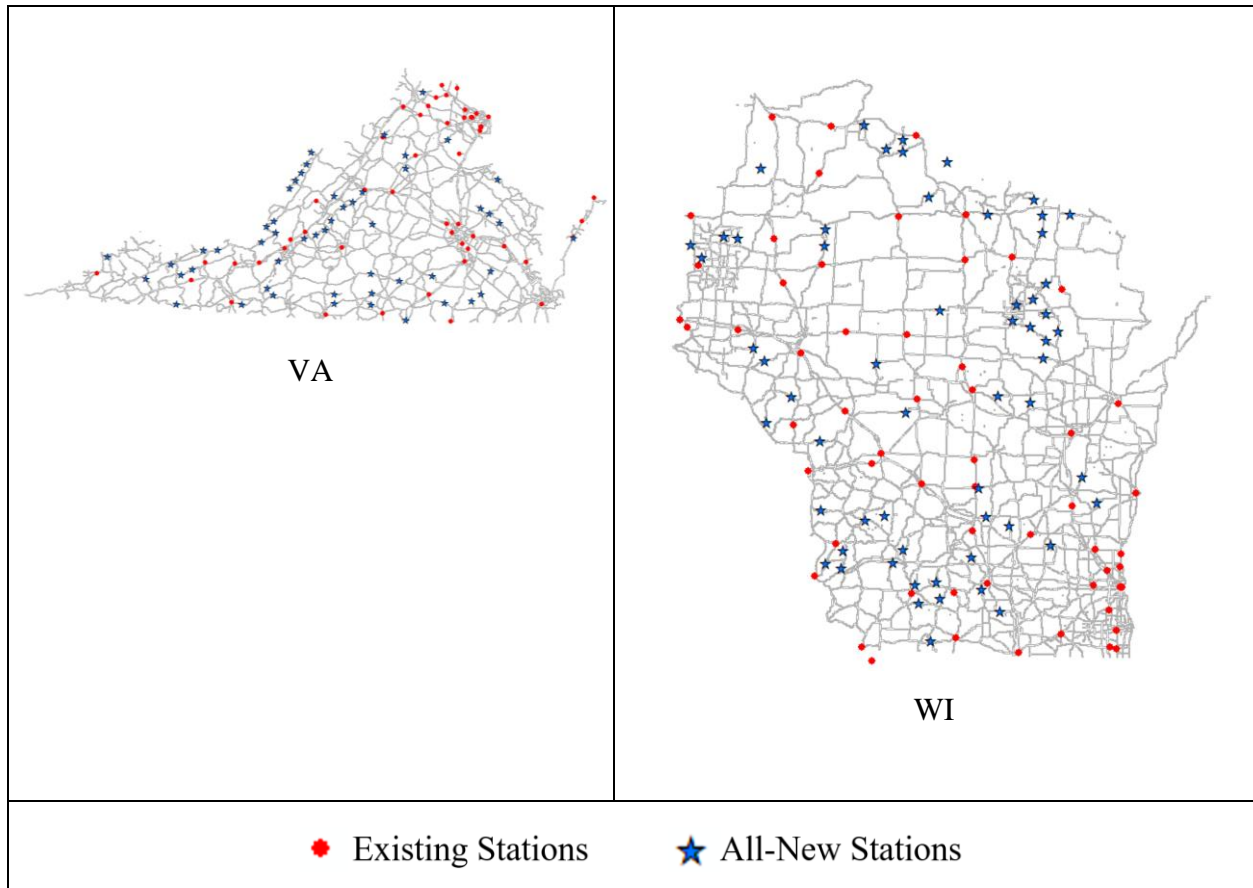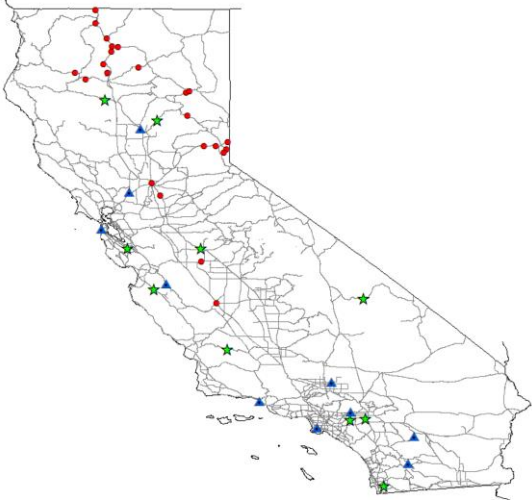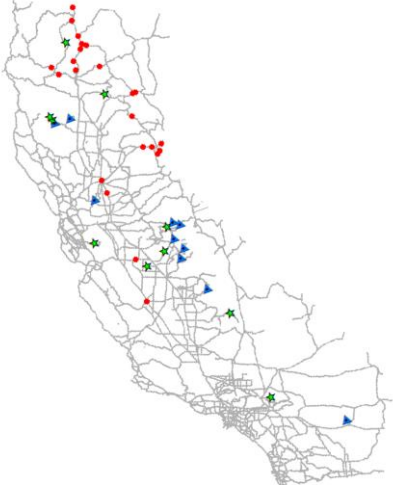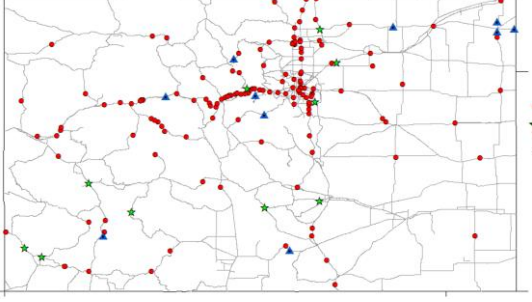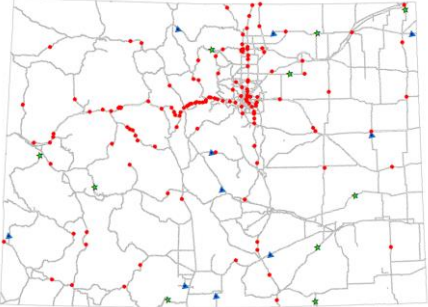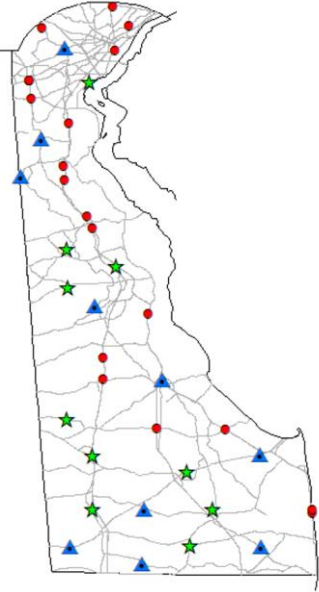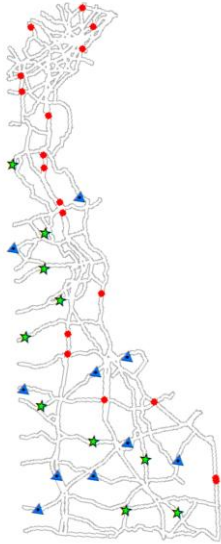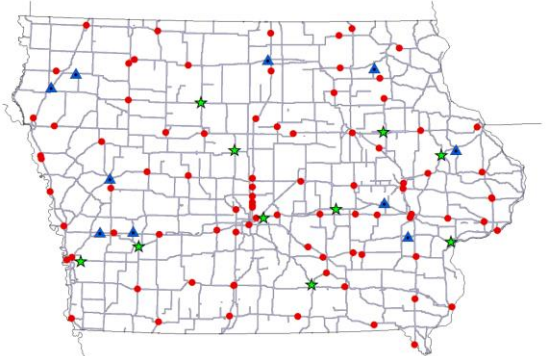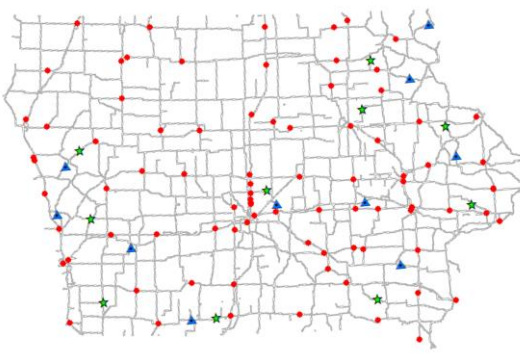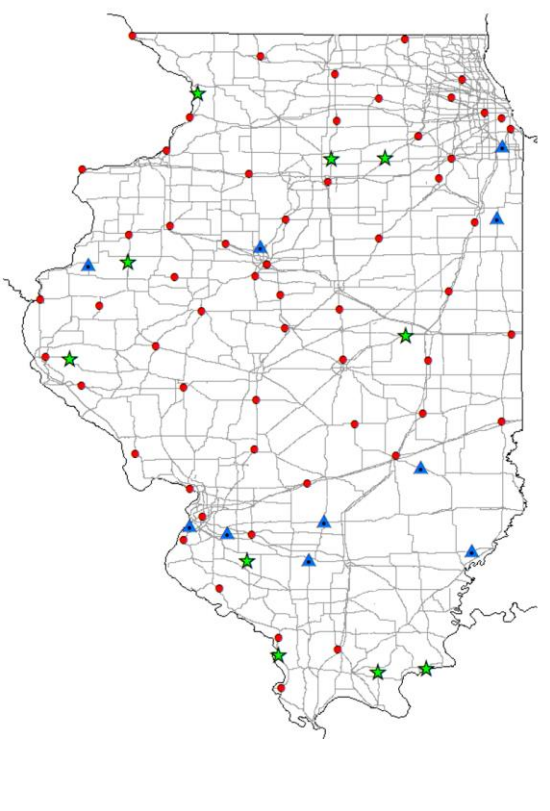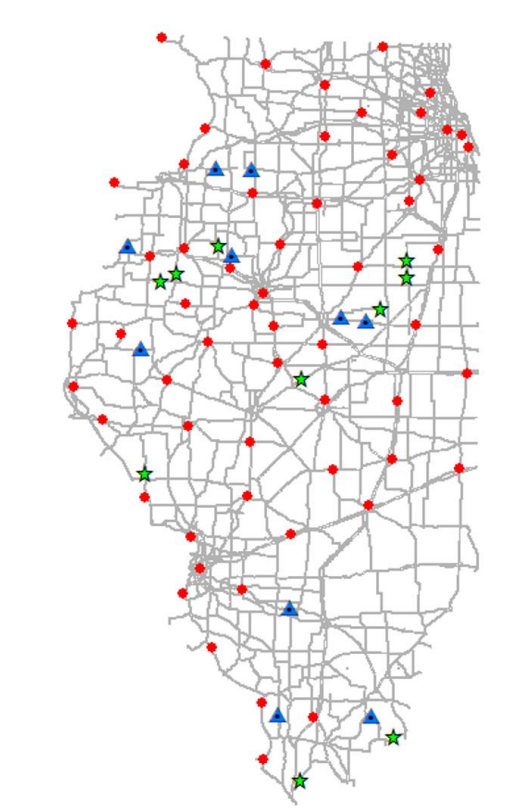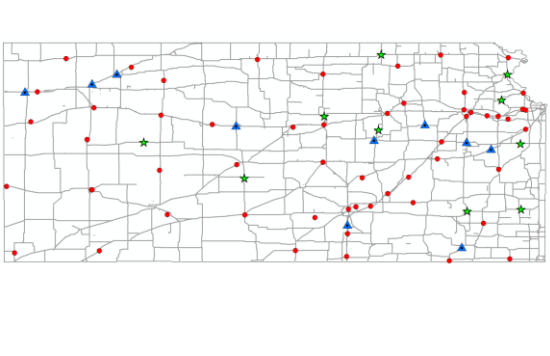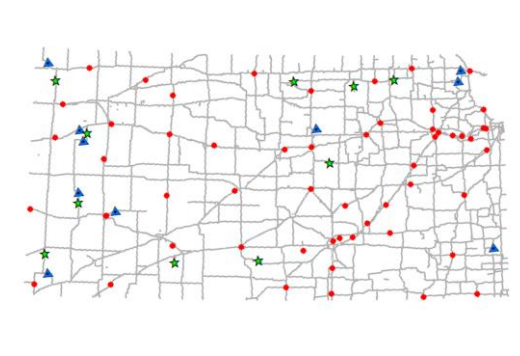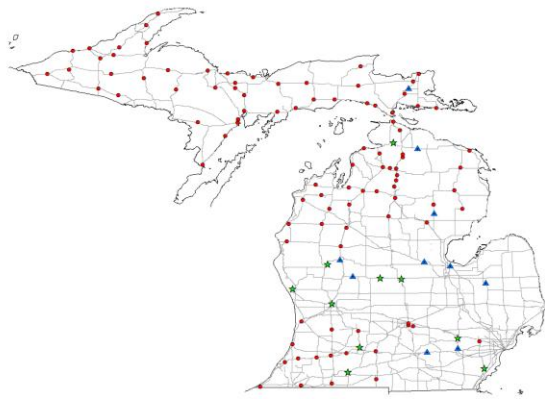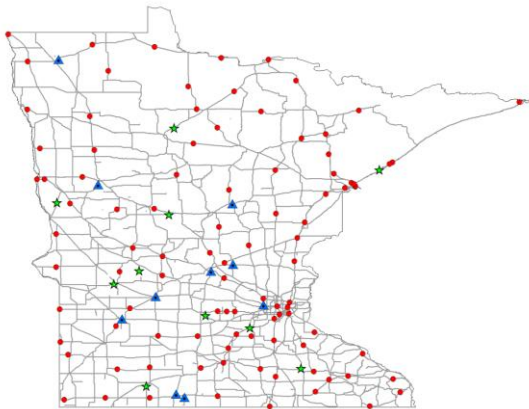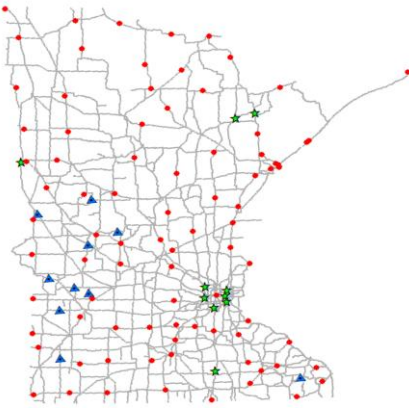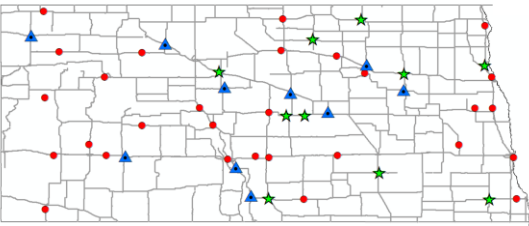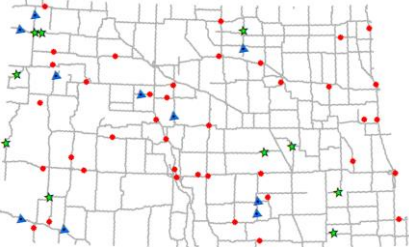
Figure 17: Existing and all-new optimized RWIS locations
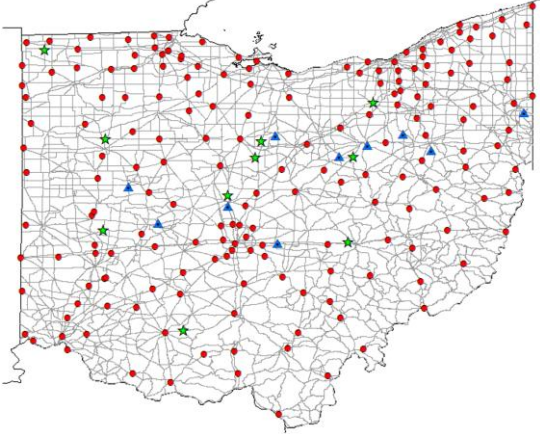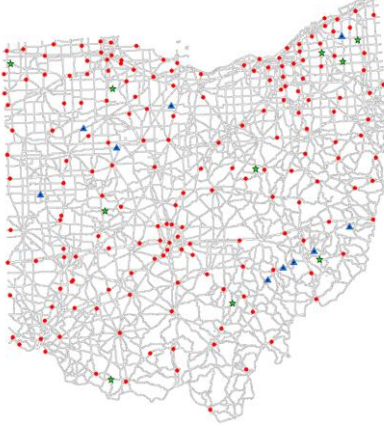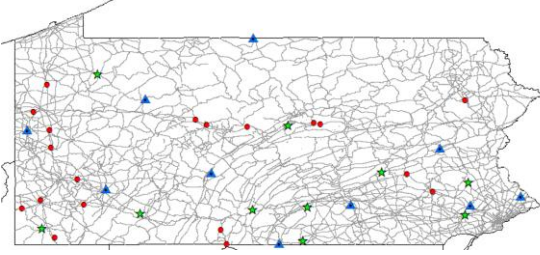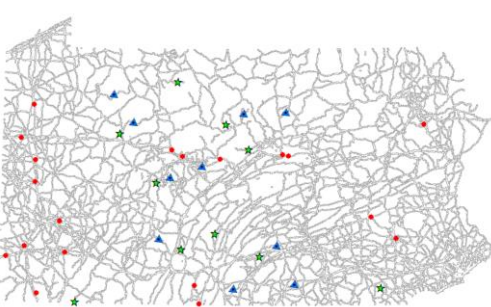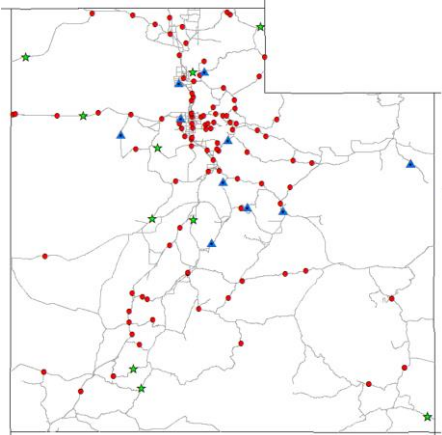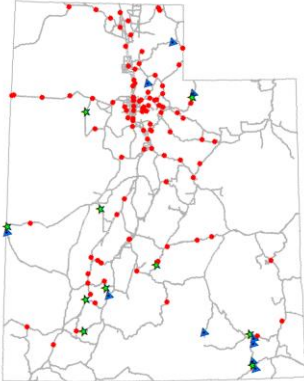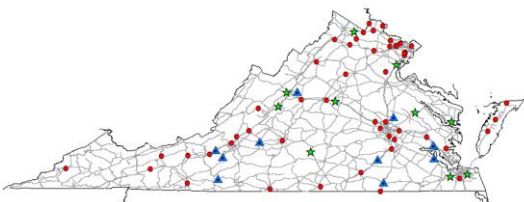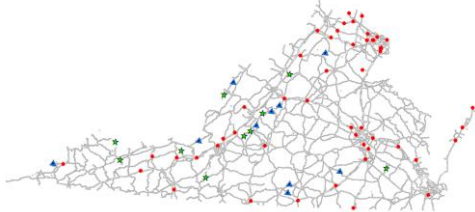
A State-wide Expansion of the Current RWIS Network

RWIS network expansion scenarios were proposed by locating a new set of 10 and 20 additional RWIS stations to the existing network of the candidate states to increase coverage and enhance winter maintenance operation program. The optimization problem has therefore been modified to include the existing stations as input and locate the additional stations accordingly. Network expansion solutions were generated considering two different criteria: (a) considering weather only and (b) considering dual criterion (both weather and traffic). Location plans for adding new stations in the existing RWIS network for study area are presented in Figure 18 and the location information is provided in Appendix B.

Region	Criteria 1 (Weather Only)	Criteria 2 (Dual Criteria)
CA		
CO		
DE		

IA		
IL		
KS		

MI		
MN		
ND		

OH	
PA	
UT	
VA	

Figure 18: Locations of existing, first 10 and second 10 additional RWIS stations considering (a) weather data only and (b) dual criteria (both weather and traffic data)

Effects of Spatial Demarcation

This section aims to evaluate how existing RWIS configurations in neighboring states influences the RWIS optimization process. In the research, IA, with 86 existing RWIS and six Border States, was selected as the study area. The methodology was applied to derive two different optimal RWIS location sets for IA under two conditions; (A) by considering the RWIS stations of bordering states' and (B) without considering the RWIS stations of bordering states'. The comparison between the developed results herein can be a good representation with respect to the effects of the bordering states' RWIS stations. Figure 19 represents the RWIS optimization process with/without considering bordering states' effects. As is evidently shown, by combining the neighboring RWIS, the derived RWIS solutions focus on urban areas.
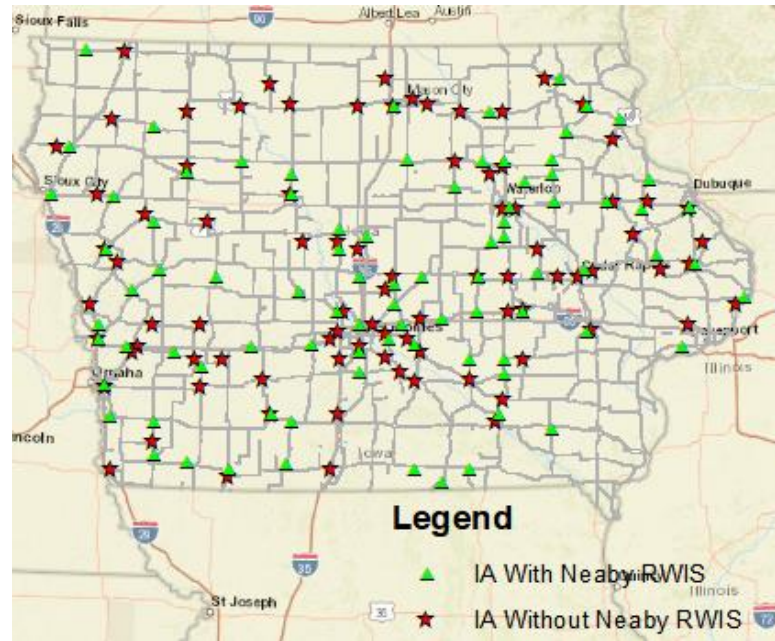
Figure 19: The RWIS optimization for IA

To statistically explain the differences, we conducted two different statistical analyses to compare the similarity between the two RWIS patterns. First is the two-sample t-statistic for the mean, which suggest the directionality of the surrounding RWIS effect. If the centroid distance between the two groups is significantly different, then the surrounding RWIS stations can be seen as having an uneven effect on the location optimization process of RWIS.

The other part is a two-sample F-statistic for variance test. This test shows the effect of nearby RWIS locations by resulting a relatively higher RWIS density in the center of the study area. The two tests evaluate the directionality and effectiveness of the surrounding RWIS location. According to the directionality test, the t-value has been found to be 0.21 meaning the effect of bordering states does not pose a directional effect. The F-test result is presented in Figure 20. The null hypothesis assumed in F-test was that, Scenario A has the same variance as B. The resulting p-value is 0.866, which suggests that we have an 86.6% probability to reject the correct null hypothesis if we would choose to reject. The F-test value is 1.273117, which lies in the 95% critical value accepted range: [0.699, ∞]. This result indicates that, Scenario A has a lower variance than B. Hence, the deployment of RWIS should take the RWIS of bordering states into consideration.
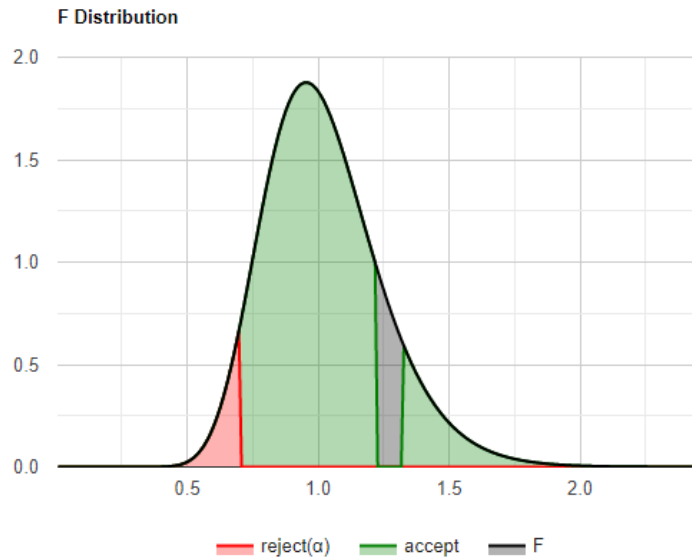
Figure 20: F-statistic distribution

4.5 RWIS Density Guidelines and Their State-wide Applications

Development of Optimal RWIS Density Guidelines

Spatial parameters of a spatiotemporal semivariogram were used as input for density optimization for topographic and weather severity zones (3 TPI classes and 4 WSI classes). A hypothetical network of 100 km × 100 km was used for density optimization. A 5 km × 5 km prediction grid was generated in ArcGIS (ESRI 2015) to create the candidate sites for RWIS station placement. The objective function was formulated to minimize the mean ordinary kriging estimation variance and solved via PSO as described earlier. The algorithm will optimize the location and density of RWIS stations in an iterative process where stations are added one by one into the study area and locations are selected based on heuristic attempts to minimize the objective function. The total number of RWIS stations allowed is arbitrarily limited to 100 in this study to ensure the variation trend of the estimation error as density changes can be fully displayed. The number of iterations is set to 5,000, after which the search process for new RWIS station locations is set to stop. Prediction errors were normalized to make a valid and fair comparison among zonal classes.

46

According to the density optimization results as shown in Figure 21, topographic and weather severity classes with larger spatial ranges required a lower number of RWIS stations, except weather zone 3, which shows a similar trend to weather zone 1. Such findings are in agreement with analyses using TPI classes: WSI 3 zone consists mainly of northern parts of MN, classified as flatland area (TPI 1) and found to have a lower density of RWIS based on topographic analyses. In addition, our density optimization is conducted using all three semivariogram parameters (range, nugget, and sill); while the dependency of the semivariogram range upon topographic-weather characteristics of the region is our main concern in this analysis. From this, it can be stated that topographic measures (TPI) provide a more intuitive and direct relationship with the impact that the spatiotemporal range has on optimal density.
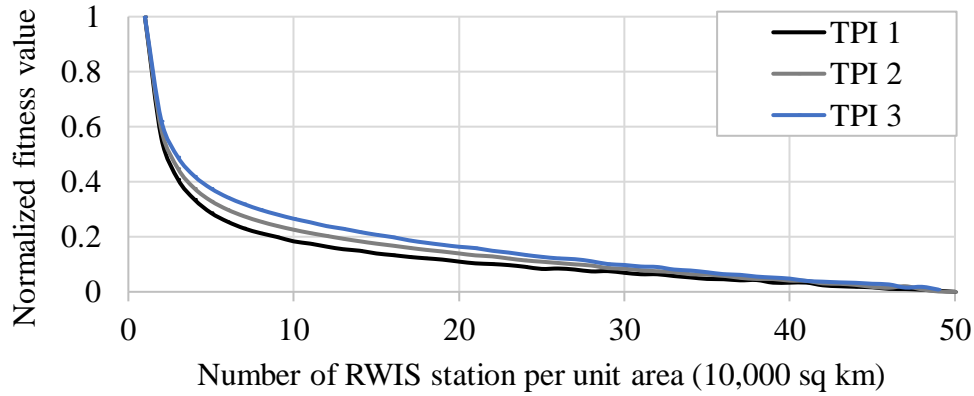
(a)
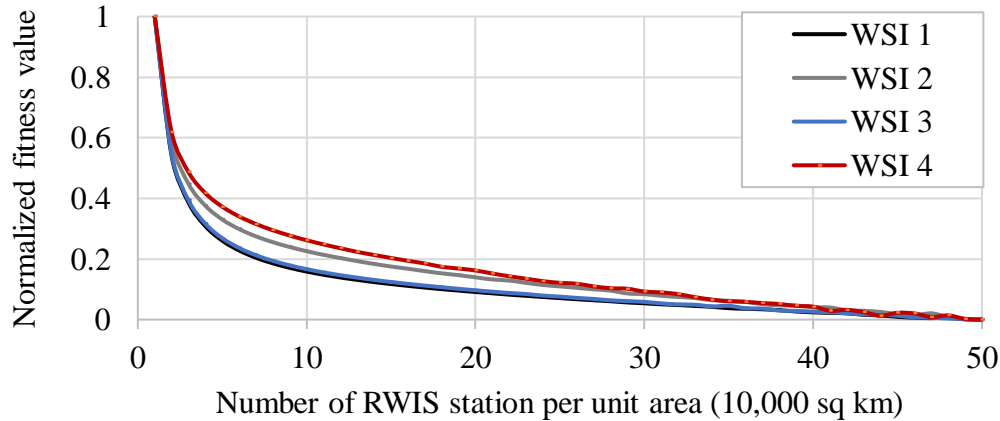
(b)

Figure 21: Normalized prediction error as a function of RWIS density for (a) TPI classes and (b) WSI classes

The number of RWIS stations needed for 0.1-unit increment of benefit is calculated from Figure 21 and presented in Figure 22. According to Figure 22, the initial 0.1-unit of incremental benefit requires the highest number of RWIS stations with each subsequent incremental benefit requiring fewer and fewer additional stations. This is as expected because the amount of marginal benefit from additional RWIS stations should decrease as station numbers increase. A similar trend is observed for both TPI and WSI classes.
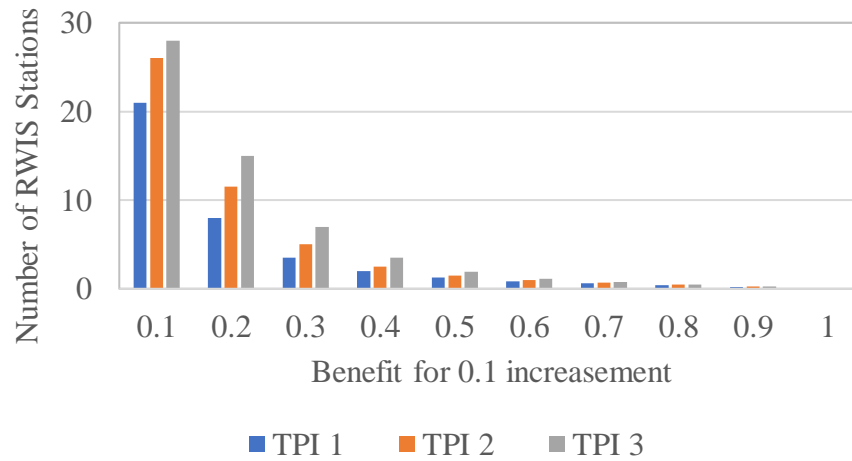
(a)
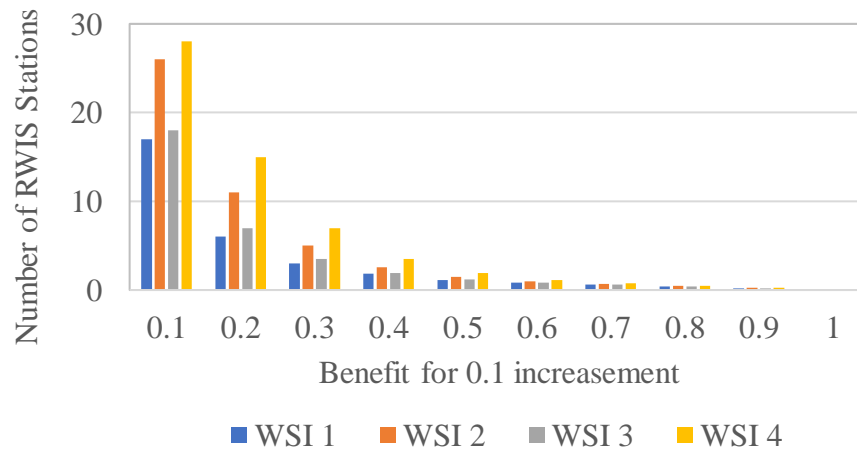
(b)

Figure 22: Number of RWIS stations for benefit increment of 0.1-unit for (a) TPI classes and (b) WSI classes

For determining the optimal RWIS density, marginal benefits are calculated from Figure 21 and presented in Figure 23. According to Figure 23, the number of added RWIS stations for an initial marginal incremental benefit of 0.1-unit is the highest and then the number of additional stations decreases for further increments of marginal benefits for both TPI and WSI classes.
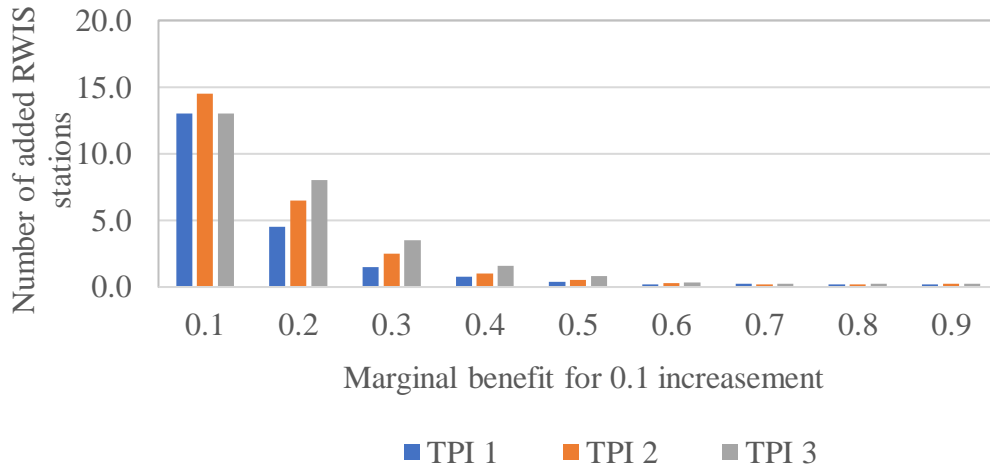
(a)
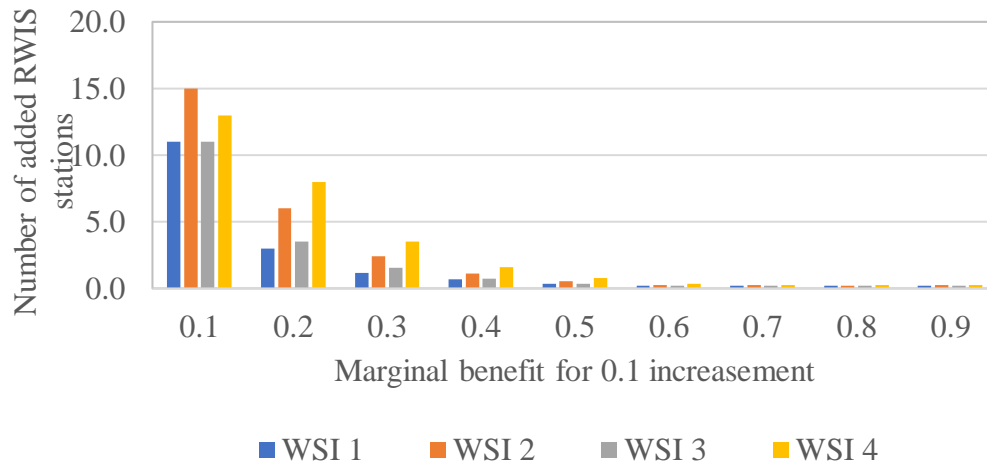
(b)

Figure 23: Added number of RWIS stations for marginal benefit increment of 0.1-unit for (a) TPI classes and (b) WSI classes

Looking at Figure 22 and Figure 23, it can be noted that the marginal benefit decreases significantly after the 0.3-unit increment of benefit mark. This is determined as the median of the range and number of associated RWIS stations for 0.3-unit increment of benefit increase is defined as the optimal RWIS density. The number of RWIS stations needed for an incremental benefit of 0.2-unit and 0.4-unit are selected as the upper and lower bound, respectively. The number of RWIS stations needed for 0.2, 0.3 and 0.4-unit benefit increment is recorded from Figure 22 and plotted in Figure 24. According to this figure, RWIS density is the lowest for TPI class 1 and increases with an increase in topographic variation. Similarly, RWIS station numbers for less weather severe regions are the lowest and increases with an increase in weather severity, except WSI 3 for the above noted reasons.

(a)

(b)

Figure 24: RWIS density comparison for (a) TPI classes and (b) WSI classes

The density optimization results are used to generate an RWIS density chart for TPI-WSI zones and is presented in Table 2. On average, three to the seven RWIS stations are required for unit area of 10,000 square km depending on the topographic feature of the landform and weather severity of the region. Such findings can readily be used by winter road maintenance agencies for planning a region-wide RWIS network, especially for regions with limited or no available RWIS stations.

Table 2: RWIS Density for TPI-WSI Zones for Unit Area (1/10000 sq km)

RWIS Density for Unit Area		TPI Classes								
		TPI 1			TPI 2			TPI 3		
		LB	Avg	UB	LB	Avg	UB	LB	Avg	UB
WSI Classes	WSI 1	1.93	3.25	7.00	2.18	4.00	8.75	2.68	5.00	10.50
	WSI 2	2.30	4.25	9.50	2.55	5.00	11.25	3.05	6.00	13.00
	WSI 3	1.98	3.50	7.50	2.23	4.25	9.25	2.73	5.25	11.00
	WSI 4	2.75	5.25	11.50	3.00	6.00	13.25	3.50	7.00	15.00

State-wide RWIS Density Determination

The optimal RWIS density was determined for each of the fourteen states using Table 2. The optimal RWIS density map is presented in Figure 25. Nine different TPI-WSI combined zones were identified in the study area. The flatland area (TPI – 1 zone) includes four different weather severity zones named as T1W1, T1W2, T1W3 and T1W4 (lighter colored area in Figure 25). Weather severity increases from southern to northern part of the study area. The optimal RWIS density in these regions varies from 3.25 to 5.25 stations per unit area (1/10000 sq km). The TPI – 2 zone, which are hilly areas, combines two different types of weather severity zones in the study area named as T2W2 and T2W2. These areas include a smaller part of KS, CO and UT. Four to five RWIS stations are needed per unit area in these zones. Mountainous areas (TPI – 3 zone) include 3 different types of weather severity zones named as T3W2, T3W3 and T3W4. A very small area of CA, CO and UT is under T3W2 and T3W3 zones. Most of the mountainous areas are under extremely high severe weather regions.

The area under each TPI-WSI zones was calculated to determine the optimal RWIS density for each state. Table 3 presents the suggested RWIS density for the 14 states. The findings from the density analyses show that the number of RWIS stations needed for adequate monitoring coverage of mountainous regions with highly varied climates (i.e., CA, CO and UT) are relatively higher than regions that are relatively flat and experience less varied weather. This makes intuitive sense since highly varied regions in terms of weather and topography would typically require more frequent monitoring of road weather and surface conditions during inclement weather events to provide timely and cost-efficient winter road maintenance operations. A suggested RWIS density for DE was found to be the lowest for having the smallest area with relatively less-varying weather and topographic conditions.

It is worthwhile noting that the values provided are for reference only and further investigation may be warranted for determining optimal densities based on different weighting schemes (i.e., traffic vs weather) and budgetary constraints since the more RWIS stations there are, the better coverage they will provide.
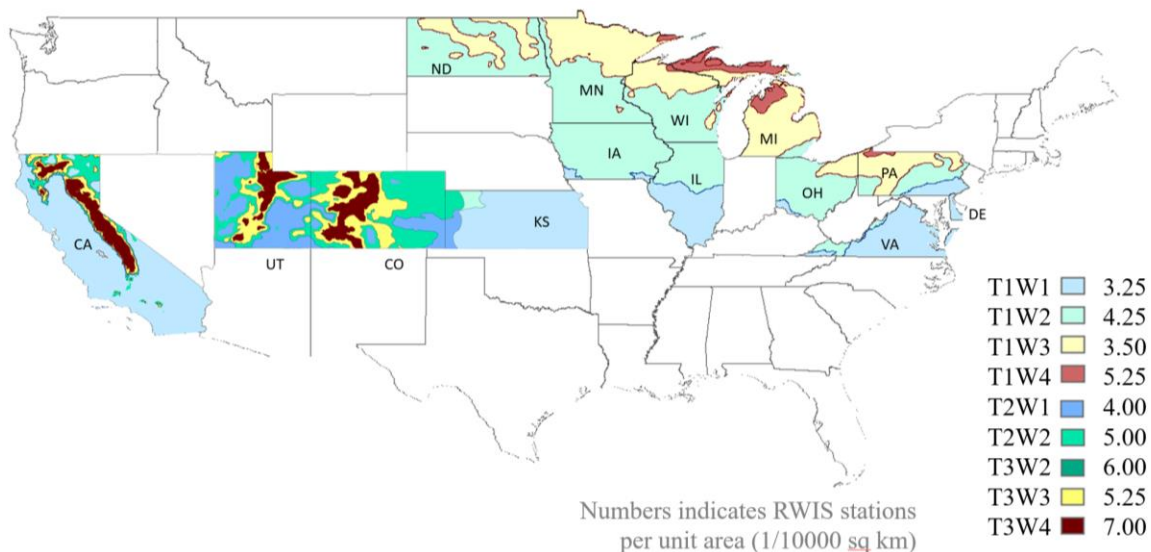
Figure 25: Optimal RWIS density map

Table 3: Suggested RWIS density for the 14 united states

States	CA	CO	DE	IA	IL	KS	MI	MN	ND	OH	PA	UT	VA	WI
RWIS Density	198	156	2	61	54	73	61	86	75	45	46	127	37	58

5. CONCLUSION AND RECOMMENDATIONS

Winter road maintenance is one of the most critical activities for transportation maintenance agencies, especially for cold region countries. The significant and critical information needed for making winter road maintenance decisions is related to road condition and weather data, which is often collected, processed, and transmitted by road weather information systems (RWIS). Effective and efficient planning of RWIS networks is a must, and is needed for maximizing the monitoring coverage and benefit of RWIS. The effectiveness of an RWIS network depends on its density and spatial distribution. In this study, we investigated the representativeness of RWIS measurements in two analysis domains – space and time. Spatial and temporal continuity of the variable of interest – *road surface temperature (RST)* were investigated using geostatistical spatiotemporal semivariogram analysis and compared to different topographic and weather regions. Lastly, optimal RWIS density for three TPI and four WSI zones were estimated from the density optimization output. The key findings of this study are listed below:

- This study examined and compared the topographic and weather features of the area under investigation. The measures used for comparing the topographic and weather characteristics of the study area were TPI and WSI, respectively. The twenty US states covered in this project were classified into three TPI classes and four WSI classes.

- A spatiotemporal analysis concluded strong dependency of spatial and temporal autocorrelation ranges of RWIS measurements with TPI and WSI values from their associated regions. The zone with the highest topographic variation (TPI class 3 mountainous region) had a shorter range of spatiotemporal structure, whereas zones with lower TPI values (TPI class 1 flatland region) had a higher range. Similarly, areas with less severe weather tended to have a higher spatial range (e.g., WSI class 1 whereas areas with more severe weather had a lower range in spatial autocorrelation).

- The RWIS location allocation framework was extended to account both spatial and temporal attributes of road weather conditions and provided more complete and conclusive location solutions. In addition, the framework reestablished in this work provides an

important basis for strategically locating regional RWIS stations, which are optimal in collecting measurements over space and time.

- A series of RWIS density curves was generated, and an optimal RWIS chart was created for the first time in literature providing a decision support tool to any transportation authorities in need of planning a RWIS network without the need for having road weather and surface conditions data.

- The desired RWIS density shows a strong dependency on topography and weather characteristics of the region under investigation. Higher RWIS density is required for regions with high topographic variation and high incidence of severe weather; while lower RWIS density is needed for less varied topographic regions with less incidence of severe weather to achieve similar levels of monitoring coverage.

- The solutions developed in this project were integrated into LoRWIS (www.lorwis.com) – a prototype web-based RWIS location visualization platform for demonstrating the proposed models and the resulting solutions.

Recommendations for further research in this direction are listed below:

- This study covers a wide region of flatland area, but the hilly and mountainous area covers a very small part of the total study area due to data availability issues. Hence, more case studies covering wider regions should be conducted for a better understanding of the relationship between spatial range of autocorrelation in RST on the topographic – weather features to develop a more robust quantitative relation between these parameters.

- The study period of this project is limited to one winter season, including six months from October 2016 to March 2017. Thus, large temporal ranges could be considered to improve the level of confidence in the outcomes.

- Universal kriging or kriging with external drift could be applied considering meteorological parameters (wind speed and direction, precipitation, humidity, cloud cover,

vegetation cover etc.) to better capture the dependency of RST data (or other key parameters including road surface condition index) on local meteorological parameters.

- Lastly, a sensitivity analysis could be conducted to investigate how the resulting optimal densities would change with respect to some of factors considered in the analysis, especially, those coefficients used to generate a winter severity index (or even a winter severity index model) and TPI classification schemes.

REFERENCES

Ahmed, S. O., R. Mazloum and H. Abou-Ali. Spatiotemporal interpolation of air pollutants in the Greater Cairo and the Delta, Egypt. Environmental research, 2018. 160, 27-34.

Andrey, J. C., B. E. Mills, and J. Vandermolen. Weather information and road safety. *Institute for Catastrophic Loss Reduction (ICLR)*, Toronto, Ontario, Canada, 2001. Paper Series – No. 15.

Biswas S., M. Wu, S. J. Melles, and T. J. Kwon. Use of Topography, Weather Zones, and Semivariogram Parameters to Optimize Road Weather Information System Station Density across Large Spatial Scales. *Transportation Research Record: Journal of the Transportation Research Board*, 2019. 0361198119846467.

Bohling, G. Introduction to geostatistics and variogram analysis. *Kansas Geological Survey*, Vol. 1, 2005, pp. 1-20.

Boselly, S. E., G. S. Doore, J. E. Thornes, C. Ulbery and D. D. Einst. *Road Weather Information Systems.* Volume 1: Research report SHRP-H-350, National Research Council, Washington D.C., USA. 1993.

Brus, D. J. and G. B. Heuvelink. Optimization of sample patterns for universal kriging of environmental variables. *Geoderma*, 2007. 138(1-2): 86-95.

Chapman, L. and J. E. Thornes. The influence of traffic on road surface temperatures: Implications for thermal mapping studies. *Meteorological Applications*, 2005. 12:371-380.

Chen, F., S. Chen and G. Peng. Using sequential gaussian simulation to assess geochemical anomaly areas of lead element. In *International Conference on Computer and Computing Technologies in Agriculture*, Springer, Berlin, Heidelberg 2012. pp. 69-76

Eriksson, M. and J. Norrman. Analysis of station locations in a road weather information system. *Meteorological Applications*, Vol. 8, No. 4, 2001, pp. 437–448.

ESRI. ArcGIS version 10.4. 1. 2015.

Gething, P. W., P. M. Atkinson, A. M. Noor, P. W. Gikandi, S. I. Hay and M. S. Nixon. A Local Space–Time Kriging Approach Applied to a National Outpatient Malaria Data Set. *Computers & Geosciences*, 2007. 33(10): 1337-1350.

Graler B., E. Pebesma and G. Heuvelink. Spatio-temporal interpolation using gstat. *RFID Journal,* 2016. 8(1), 204-218.

Gu, L., M. Wu and T. J. Kwon. An Enhanced Spatial Statistical Method for Continuous Monitoring of Winter Road Surface Conditions. *Canadian Journal of Civil Engineering*, (ja), 2019.

Gustavsson, T. Variation in road surface temperature due to topography and wind. *Theoretical and Applied Climatology,* 1990. 41:227-236.

Hastie, T. J. and R. J. Tibshirani Generalized Additive Models. Chapman & Hall/CRC, 1990.

Heuvelink, G. B., D. J. Brus and J. J. de Gruijter. Optimization of sample configurations for digital mapping of soil properties with universal kriging. *Developments in Soil Science*, 2006. 31: 137-151.

Hu, D., H. Shu, H. Hu and J. Xu. Spatiotemporal regression Kriging to predict precipitation using time-series MODIS data. Cluster Computing, 2017. 20(1), 347-357.

Jenness, J. (2006). Topographic position index (TPI) v. 1.2. Flagstaff, AZ: *Jenness Enterprises*.

Jin, P., A. Walker, M. Cebelak and C. Walton. (2014). Determining strategic locations for environmental sensor stations with weather-related crash data. *Transportation Research*

Record: Journal of the Transportation Research Board, No. 2440, Transportation Research Board of the National Academics, Washington, D.C., 2014, pp. 34-42.

Kennedy, J. and R. Eberhart. Particle Swarm Optimization. In IEEE International Conference on Neural Networks.1995. pp. 1942–1948. doi:10.1109/ICNN.1995.488968.

Kennedy, J. and R.C. Eberhart. A Discrete Binary Version of the Particles Swarm Algorithm. In Systems, Man, and Cybernetics, Computational Cybernetics and Simulation, IEEE International Conference. 1997. pp. 4–8. doi:10.1109/ICSMC.1997.637339.

Kwon, T. J. and L. Fu. Evaluation of alternative criteria for determining the optimal location of RWIS stations. *Journal of Modern Transportation*, Vol. 21, No. 1, 2013, pp. 17–27.

Kwon, T. J., and L. Fu. *RWIS network planning: Optimal density and location*. 2016. (No. Aurora Project 2010-04).

Kwon, T. J., L. Fu and S. J. Melles. Location optimization of road weather information system (RWIS) network considering the needs of winter road maintenance and the traveling public. *Computer-Aided Civil and Infrastructure Engineering*, Vol. 32, No. 1, 2017, pp. 57–71.

Kwon, T. J. and L. Fu. Spatiotemporal variability of road weather conditions and optimal RWIS density—an empirical investigation. *Canadian Journal of Civil Engineering*, Vol. 44, No. 9, 2017, pp. 691–699.

Kirkpatrick, S., C. D. Gelatt and M. P. Vecchi. Optimization by simulated annealing. *Science*, 1983. 220(4598): 671-680.

Li, L., J. Zhang, W. Qiu, J. Wang and Y. Fang. An ensemble spatiotemporal model for predicting PM2. 5 concentrations. *International journal of environmental research and public health*, 2017. 14(5), 549.

Lichtenstern, A. Kriging methods in spatial statistics. 2013.

Manfredi, J., T. Walters, G. Wilke, L. Osborne, R. Hart, T. Incrocci, and T. Schmitt. *Road Weather Information System Environmental Sensor Station Sitting Guidelines.* Publication No. FHWA-HOP-05-026. Federal Highway Administration. 2005.

Manfredi, J., T. Walters, G. Wilke, L. F. Osborne, R. Hart, T. Incrocci and C. Schmitt. *Road Weather Information System Environmental Sensor Station Siting Guide*, Version 2.0. No. FHWA-HOP-05-026. United States Department of Transportation, 2008.

Matthews, L., J. Andrey, I. Minokhin and M. Perchanok. *Operational Winter Severity Indices in Canada–From Concept to Practice*. Presented at 96th Annual Meeting of the Transportation Research Board, Washington, D.C., 2017.

Matthews, L., J. Andrey, D. Hambly and I. Minokhin. Development of a flexible winter severity index for snow and ice control. *Journal of Cold Regions Engineering*, Vol. 31, No. 3, 2017, p. 04017005.

Mewes, J. J. Mapping weather severity zones (No. CR10-02). 2011.

Mokarram, M., G. Roshan and S. Negahban. Landform classification using topography position index (case study: salt dome of Korsia-Darab plain, Iran). *Modeling Earth Systems and Environment*, 2015. 1(4): 40.

Network, R. E. S. S. T. E. Analyzing spatio-temporal data with R: Everything you always wanted to know–but were afraid to ask. Submitted to *Journal de la Société Française de Statistique*, 2016.

Olea, R. A. A six-step practical approach to semivariogram modeling. *Stochastic Environmental Research and Risk Assessment*, Vol. 20, No. 5, 2006, Pp. 307-318.

Olea, R. A. *Geostatistics for engineers and earth scientists*. Springer Science & Business Media, New York, 2012.

Pebesma, E.J. Multivariable geostatistics in S: the gstat package. *Computers & Geosciences*, Vol. 30, 2004, pp. 683–691.

Pebesma, E. and B. Graeler. Spatial and spatio-temporal geostatistical modelling, prediction and simulation. 2012.

Pebesma, E. and Gräler, B. Introduction to Spatio-Temporal Variography. 2018.

Pebesma, E., B. Graeler and M. E. Pebesma. Package 'gstat'. 2019.

Poli, R., J. Kennedy and B. Tim. Particle swarm optimization. *Swarm Interlligence*, 1: 33–57. 2007. doi:10.1007/s11721-007-0002-0 Particle.

R Core Team. *R: A language and environment for statistical computing*. R Foundation for Statistical Computing, Vienna, Austria, 2018. URL https://www.R-project.org/.

Revelle, C. S., H. A. Eiselt and M. S. Daskin. A bibliography for some fundamental problem categories in discrete location science. *European Journal of Operational Research*, 2008. 184(3): 817-848.

Seif, A. Using Topography Position Index for Landform Classification (Case study: Grain Mountain). *Bulletin of Environment, Pharmacology and Life Sciences (Bull. Env. Pharmacol. Life Sci)*, 2014. 3: 33-39.

Seif, A. Landform Classification by Slope Position classes. *Bulletin of Environment, Pharmacology and Life Sciences*, Vol. 3, 2014, pp. 62–69.

Shacklette, M. Linux Operating System. *Handbook of Computer Networks: LANs, MANs, WANs, the Internet, and Global, Cellular, and Wireless Networks*, 2, 78-90. 2007.

Shekhar, S., H. Xiong and X. Zhou Encyclopedia of GIS. Springer, New York, 2008.

Shi, Y. Particle swarm optimization: developments, applications and resources. In *Proceedings of the 2001 congress on evolutionary computation* (IEEE Cat. No. 01TH8546), 2001. (Vol. 1, pp. 81-86). IEEE.

Solana-Gutiérrez, J. and S. Merino-de-Miguel. A Variogram Model Comparison for Predicting Forest Changes. *Procedia Environmental Sciences*, Vol. 7, 2011, pp. 383-388.

Van Groenigen, J. W. and A. Stein. Constrained optimization of spatial sampling using continuous simulated annealing. *Journal of Environmental Quality*, 1998. 27(5): 1078-1086.

Van Groenigen, J. W., W. Siderius and A. Stein. Constrained optimisation of soil sampling for minimisation of the kriging variance. *Geoderma*, 1999. 87(3-4): 239-259.

Wang, H., H. Sun, C. Li, S. Rahnamayan and J. S. Pan. Diversity enhanced particle swarm optimization with neighborhood search. *Information Sciences*, 223: 119–135. Elsevier Inc. 2013. doi:10.1016/j.ins.2012.10.012.

Wang, X., L. Gu, T. J. Kwon and T. Z. Qiu. Determining the Spatiotemporal Coverage of Road Weather Information Systems–A Case Study in Alberta, Canada. *Transportation Research Record: Journal of the Transportation Research Board*, 2019. (No. 19-00551).

Weiss, A. Topographic Positions and Landforms Analysis (Conference Poster). *ESRI International User Conference*. San Diego, CA, 2001. pp. 9-13.

White, S. P., J. E. Thornes and L. Chapman. *A Guide to Road Weather Information Systems*. Version 2. SIRWEC, University of Birmingham, UK. 2006, pp. 1–83.

Appendix A – All-New Optimized RWIS Network (lat/long)

Table 4: Location of all-new RWIS stations – using dual criterion (considering both weather and traffic data)

CA:

Station Number	Longitude	Latitude	Station Number	Longitude	Latitude	Station Number	Longitude	Latitude
1	-117.28	34.26	9	-120.22	39.67	17	-122.22	40.12
2	-121.51	37.34	10	-119.57	37.31	18	-121.61	40.05
3	-122.67	41.25	11	-122.41	41.01	19	-117.87	34.81
4	-122.02	40.31	12	-118.11	34.31	20	-120.39	36.97
5	-122.36	39.55	13	-117.64	35	21	-115.96	32.87
6	-116.25	32.66	14	-119.38	37.21	22	-117.83	34.34
7	-119.31	37.43	15	-121.71	42.01	23	-119.6	37.75
8	-119.98	37.63	16	-119.37	37.33			

CO:

Station Number	Longitude	Latitude	Station Number	Longitude	Latitude	Station Number	Longitude	Latitude
1	-106.44	38.13	50	-103.31	40.52	99	-105.55	39.67
2	-107.8	37.66	51	-102.96	40.29	100	-105.71	39.04
3	-105.19	37.79	52	-105.74	40.71	101	-105.08	38.28
4	-103.12	40.88	53	-106.13	39.72	102	-106.58	39.13
5	-107.67	37.17	54	-104.31	40.08	103	-105.78	39.81
6	-102.5	38.44	55	-103.6	40.53	104	-107.84	40.18
7	-102.66	40.64	56	-103.14	40.61	105	-103.71	38.23
8	-108.26	40.44	57	-103.48	38.27	106	-104.55	40.62
9	-104.08	40.35	58	-105.61	39.63	107	-104.37	40.08
10	-108.31	40.13	59	-104.34	37.24	108	-103.01	40.42
11	-104.28	37.33	60	-105.89	39.68	109	-103.7	38.59
12	-102.95	38.8	61	-104.49	40.48	110	-106.03	40.53

13	-102.97	40.11	62	-106.77	37.5	111	-105.42	38.05
14	-106.49	40.3	63	-102.96	40.24	112	-105.08	39.04
15	-103.31	38.09	64	-107.08	38.39	113	-103.66	40.61
16	-107.62	40.46	65	-102.23	40.77	114	-106.19	39.81
17	-103.49	40.25	66	-108.69	40.7	115	-108.49	38.95
18	-106.27	37.64	67	-104.73	39.18	116	-105.02	37.96
19	-105.14	38.1	68	-102.97	40.02	117	-103.87	38.18
20	-105.87	37.69	69	-103.18	38.85	118	-105.49	40.13
21	-102.79	40.15	70	-106.1	38.09	119	-102.75	39.65
22	-102.56	38.44	71	-104.61	40.58	120	-108.19	40.08
23	-103.2	37.86	72	-106.34	38.45	121	-107.79	40.27
24	-104.84	40.08	73	-108.66	38.04	122	-103.62	39.53
25	-105.14	38.82	74	-105.58	38.37	123	-106.6	40.07
26	-106.85	38.54	75	-104.61	40.48	124	-103.2	37.91
27	-103.7	38.54	76	-103.9	40.3	125	-105.48	37.19
28	-103.7	38.86	77	-106.18	39.36	126	-102.1	38.47
29	-105.01	39.4	78	-103.37	40.43	127	-107.69	37.93
30	-108.67	38.22	79	-103.83	37.78	128	-108.5	38.23
31	-102.3	40.63	80	-105.43	39.99	129	-102.79	38.48
32	-103.43	37.77	81	-102.73	38.39	130	-103.01	40.79
33	-103.69	39.18	82	-107.38	40.51	131	-105.59	37.65
34	-108.84	38.03	83	-102.76	37.41	132	-105.49	38.68
35	-105.53	37.11	84	-103.53	38.05	133	-108	38.6
36	-107.7	39.65	85	-103.7	38.95	134	-108.97	38.35
37	-106.96	40.29	86	-102.72	40.33	135	-105.85	40.3
38	-107.3	38.04	87	-103.29	38.85	136	-103.64	38.86
39	-105.94	39.17	88	-103.72	40.61	137	-107.19	38.48
40	-108.16	38.06	89	-108.66	40.16	138	-102.12	37.93
41	-103.6	40.48	90	-104.21	39.09	139	-103.03	40.15
42	-105.07	38.01	91	-102.25	40.32	140	-103.33	37.28
43	-105.49	39.9	92	-106.31	37.1	141	-102.82	39.3
44	-102.87	39.52	93	-105.72	39.76	142	-103.73	40.26
45	-105.36	38.15	94	-103.21	40.07	143	-105.48	38.46

46	-103.3	38.4	95	-105.76	38.37	144	-107.45	38.93
47	-106.94	37.18	96	-104.63	37.69	145	-107.97	39
48	-105.3	37.52	97	-106.78	40.07	146	-105.38	40.17
49	-104.84	40.58	98	-108.94	37.85	147	-103.7	38.81

DE:

Station Number	Longitude	Latitude	Station Number	Longitude	Latitude	Station Number	Longitude	Latitude
1	-75.65	39.15	8	-75.24	38.82	15	-75.64	38.51
2	-75.59	39.06	9	-75.3	38.53	16	-75.36	38.78
3	-75.42	38.47	10	-75.19	38.52	17	-75.61	39.46
4	-75.71	39.37	11	-75.48	38.88	18	-75.71	38.97
5	-75.65	38.83	12	-75.3	38.65	19	-75.37	38.92
6	-75.47	38.61	13	-75.65	39.24			
7	-75.53	39.33	14	-75.51	38.99			

IA:

Station Number	Longitude	Latitude	Station Number	Longitude	Latitude	Station Number	Longitude	Latitude
1	-91.02	42.19	30	-94.96	42.42	59	-93.74	41.08
2	-93.58	41.29	31	-93.82	40.89	60	-95.49	41.69
3	-90.84	41.96	32	-93.27	41.76	61	-95.32	42.32
4	-94.58	41.52	33	-93.62	42.88	62	-95.65	42.99
5	-92.72	41.85	34	-91.35	43.19	63	-93.32	42.34
6	-95.54	41.61	35	-93.79	42.3	64	-93.62	42.97
7	-94.16	41.89	36	-93.33	41.47	65	-95.96	41.77
8	-92.17	41.76	37	-95.08	42.42	66	-95.61	40.87
9	-92.35	41.57	38	-91.54	42.88	67	-95.86	41
10	-94.47	42.2	39	-96.19	43.47	68	-95.48	41.78
11	-90.6	42.01	40	-92.25	41.84	69	-95.87	41.9
12	-93.8	42.39	41	-90.61	42.11	70	-92.01	43.47

13	-94.45	41.78	42	-95.91	42.08	71	-94.53	42.52
14	-92.53	41.58	43	-91.87	42.29	72	-91.02	42.06
15	-92.95	41.31	44	-95.74	42.23	73	-91.78	42.76
16	-95	41.65	45	-95.34	41.42	74	-93.19	41.14
17	-94.67	40.76	46	-94.72	40.71	75	-92.03	42.97
18	-92.65	40.63	47	-95.44	40.87	76	-90.72	41.65
19	-93.85	41.35	48	-92.24	41.94	77	-94.24	40.75
20	-94.72	42.83	49	-94.54	42.77	78	-94.58	41.85
21	-91.8	41.75	50	-95.74	41.95	79	-92.01	40.67
22	-95.46	42.94	51	-95.4	41.24	80	-94.98	41.25
23	-92.23	41.44	52	-95.55	42.05	81	-91.14	42.01
24	-94.98	41.34	53	-94.73	40.98	82	-93.79	40.68
25	-91.77	40.62	54	-94.83	42.42	83	-95.68	43.44
26	-92.26	42.83	55	-91.48	42.87	84	-94.02	40.72
27	-91.9	42.01	56	-94.79	41.25	85	-92.34	42.2
28	-96.5	42.81	57	-92.58	42.84	86	-91.29	42.88
29	-90.91	41.74	58	-93.6	40.77			

IL:

Station Number	Longitude	Latitude	Station Number	Longitude	Latitude	Station Number	Longitude	Latitude
1	-89.91	41.45	21	-90.65	41.07	41	-88.19	38.26
2	-90.87	40.95	22	-88.54	37.64	42	-88.18	37.56
3	-90.73	39.99	23	-89.32	41.23	43	-90.09	39.64
4	-88.37	38.67	24	-88.87	41.75	44	-88.27	38.37
5	-88.87	39.34	25	-88.84	37.51	45	-88.18	40.41
6	-89.88	39.07	26	-88.51	40.57	46	-89.4	38.77
7	-89.98	42.02	27	-88.03	39.16	47	-90.18	41.2
8	-89.74	39.63	28	-89.26	41.49	48	-89.27	37.14
9	-89.73	41.56	29	-89.34	41.02	49	-88.2	41
10	-88.45	38.08	30	-90.63	40.23	50	-87.52	38.73
11	-87.93	41.06	31	-88.58	40.48	51	-88.18	37.96

12	-88.49	37.4	32	-90.42	39.32	52	-88.73	37.46
13	-87.83	39.63	33	-89.13	41.68	53	-88.42	41.47
14	-90.12	40.22	34	-88.26	40.75	54	-90.76	39.32
15	-89.48	38.14	35	-89.17	38.94	55	-88.82	40.51
16	-88.75	37.29	36	-90.07	41.55	56	-90.63	39.36
17	-88.75	39.67	37	-87.99	39.3	57	-90.82	40.77
18	-89.13	41.44	38	-90.37	40.57	58	-89.68	40.93
19	-89.32	37.63	39	-90.64	39.46	59	-88.94	38.95
20	-87.7	40.51	40	-88.07	40.6			

KS:

Station Number	Longitude	Latitude	Station Number	Longitude	Latitude	Station Number	Longitude	Latitude
1	-100.87	37.51	20	-101.27	38.13	39	-101.18	39.03
2	-98.03	38.52	21	-98.02	39.67	40	-101.09	39.8
3	-101.06	39.13	22	-98.33	39.99	41	-95.87	38.09
4	-97.71	37.16	23	-95.72	38.54	42	-96.8	38.74
5	-97.85	39.69	24	-96.9	38.89	43	-96.47	37.25
6	-98.18	37.96	25	-101.36	37.15	44	-95.59	38.58
7	-95.91	37.78	26	-95.57	37.39	45	-101.37	39.36
8	-96.35	37.36	27	-101.27	38.27	46	-96.05	38.78
9	-99.77	37.4	28	-101.55	39.74	47	-98.58	37.5
10	-101.72	39.61	29	-98.69	37.27	48	-98.56	39.8
11	-101.75	38.75	30	-101.69	37.26	49	-96.22	37.19
12	-98.57	38.16	31	-96.69	38.96	50	-97.86	39.89
13	-101.76	37.49	32	-101.85	39.83	51	-95.14	39.43
14	-97.21	39.81	33	-101.75	38.94	52	-95.85	37.4
15	-101.72	39.11	34	-96.98	39.63	53	-94.82	37.96
16	-99.72	38.81	35	-101.1	37.49	54	-97.35	38.68
17	-101.24	38.9	36	-97.12	38.83	55	-96.65	37.05
18	-96.33	39.7	37	-100.84	37.28	56	-97.98	39.19
19	-101.77	38.12	38	-98.43	37.47			

MI:

Station Number	Longitude	Latitude	Station Number	Longitude	Latitude	Station Number	Longitude	Latitude
1	-86.18	44.7	34	-89.56	46.43	67	-87.17	46.06
2	-83.14	43.99	35	-84.17	43.92	68	-85.23	41.94
3	-84.57	44.66	36	-85.42	46.52	69	-85.74	45.04
4	-85.93	41.92	37	-85.63	44.95	70	-84.62	44.18
5	-84.51	42.34	38	-84.19	45.98	71	-84.21	45.23
6	-85.71	44.22	39	-84.65	45.86	72	-84.23	41.82
7	-84.95	43.18	40	-82.77	43.99	73	-85.14	42.49
8	-84.23	42.84	41	-83.77	44.46	74	-84.81	42.1
9	-84.03	43	42	-82.93	43.46	75	-85.18	46.61
10	-85.9	44.66	43	-83.56	44.66	76	-82.8	43.81
11	-82.91	44.04	44	-85.19	44.34	77	-87.1	46.35
12	-83.34	43.87	45	-85.08	42.94	78	-83.93	44.72
13	-85.17	44.34	46	-83.37	43.34	79	-84.75	41.7
14	-87.31	46.26	47	-83.83	44.78	80	-83.97	45.97
15	-83.68	43.23	48	-85.15	43.68	81	-85.02	46.23
16	-85.02	42.44	49	-84.83	45.99	82	-85.06	45.46
17	-85.49	44.98	50	-82.94	43.6	83	-83.77	44.92
18	-82.68	43.89	51	-86.72	46.36	84	-83.76	44.69
19	-85.08	43.31	52	-83.32	43.56	85	-84.17	45.07
20	-85.18	44.49	53	-86.1	42.1	86	-85.26	42.59
21	-85.92	44.81	54	-82.56	42.58	87	-84.7	42.37
22	-83.74	44.65	55	-84.71	45.44	88	-85.82	43.67
23	-84.46	45.51	56	-84.96	44.03	89	-83.55	43.57
24	-84.42	44.54	57	-84.75	41.85	90	-85.32	42.38
25	-85.27	43.38	58	-85.06	44.34	91	-85.93	44.93
26	-84.88	42.57	59	-85.8	44.95	92	-84.09	42.64
27	-89.56	46.72	60	-83.7	45.15	93	-85.06	46.64
28	-84.41	41.86	61	-85.82	44.12	94	-84.34	42.66
29	-82.62	43.74	62	-86.62	45.73	95	-84.04	42.22

30	-83.03	43.41	63	-85.86	42.42	96	-84.03	42.2
31	-85.1	45.09	64	-83.75	44.59	97	-84.07	42.37
32	-85.85	43.78	65	-85.1	46.49	98	-87.24	46.18
33	-84.24	46.08	66	-84.23	45.41			

MN:

Station Number	Longitude	Latitude	Station Number	Longitude	Latitude	Station Number	Longitude	Latitude
1	-95.83	48.12	30	-95.47	46.37	59	-94.09	45.86
2	-92.93	47.03	31	-96.53	46.39	60	-96.17	45.00
3	-92.50	44.29	32	-95.38	44.22	61	-92.88	46.71
4	-94.00	44.37	33	-92.86	47.84	62	-96.38	45.27
5	-95.86	45.28	34	-93.48	47.84	63	-95.47	44.98
6	-95.31	44.04	35	-93.17	47.22	64	-94.99	43.77
7	-95.92	45.10	36	-96.22	43.57	65	-95.77	45.83
8	-95.40	46.15	37	-94.70	46.57	66	-95.84	45.87
9	-93.88	44.10	38	-96.00	45.28	67	-95.56	45.43
10	-92.68	46.27	39	-94.19	44.41	68	-93.19	47.75
11	-96.43	46.04	40	-95.91	44.88	69	-96.93	47.82
12	-92.38	44.28	41	-93.12	43.87	70	-94.76	44.05
13	-95.98	43.57	42	-97.11	48.31	71	-95.67	46.55
14	-95.91	44.79	43	-95.33	46.33	72	-95.77	44.79
15	-95.75	44.07	44	-93.12	47.85	73	-95.13	44.36
16	-93.74	43.97	45	-96.28	44.64	74	-94.56	48.60
17	-93.27	47.81	46	-96.27	47.79	75	-96.43	45.01
18	-91.69	43.78	47	-94.10	46.04	76	-95.20	45.71
19	-95.12	44.04	48	-96.49	45.90	77	-95.31	47.14
20	-96.42	48.15	49	-95.44	44.40	78	-93.45	46.22
21	-93.27	46.45	50	-93.20	47.43	79	-96.71	46.47
22	-93.76	43.89	51	-94.62	43.65	80	-95.72	46.11
23	-95.00	47.78	52	-93.75	48.51	81	-94.55	48.28
24	-95.72	45.11	53	-92.41	46.49	82	-93.13	46.45

25	-96.44	47.30	54	-96.30	45.01	83	-95.94	44.16
26	-96.09	45.82	55	-93.20	48.06	84	-95.53	46.43
27	-94.70	48.77	56	-92.00	44.11	85	-96.78	45.66
28	-91.83	43.79	57	-93.67	47.84	86	-94.68	44.05
29	-94.09	45.77	58	-93.57	44.38			

ND:

Station Number	Longitude	Latitude	Station Number	Longitude	Latitude	Station Number	Longitude	Latitude
1	-99.56	46.51	11	-100.88	47	21	-103.14	46.17
2	-99.56	48.86	12	-98.43	47.1	22	-103.53	48.58
3	-98.76	48.41	13	-103.39	48.58	23	-103.37	46.42
4	-100.94	47.15	14	-99.66	48.99	24	-103.95	48.89
5	-103.15	48.05	15	-102.35	47.15	25	-103.65	47.76
6	-99.2	47.15	16	-102.78	47.1	26	-101.06	47.82
7	-103.14	46.26	17	-99.18	46.53	27	-97.82	46.63
8	-99.74	48.07	18	-102.79	46.81	28	-98.73	47.23
9	-101.33	46.23	19	-101.33	46.07	29	-98.65	47.68
10	-103.22	48.18	20	-103.16	46.52			

OH:

Station Number	Longitude	Latitude	Station Number	Longitude	Latitude	Station Number	Longitude	Latitude
1	-84.06	40.19	62	-84.26	40.49	123	-82.61	40.4
2	-84.43	41.44	63	-83.87	41.09	124	-84.35	40.05
3	-81.37	40.24	64	-81.12	40.35	125	-82.07	40.23
4	-83.9	40.29	65	-81.36	39.74	126	-84.22	41.31
5	-80.82	40.41	66	-81.13	41.31	127	-80.78	41.68
6	-83.99	41.1	67	-84.37	40.27	128	-83.72	40.25
7	-82.26	40.95	68	-83.2	38.95	129	-84.72	41.3
8	-81.84	40.23	69	-83.98	39.43	130	-84.78	39.37

9	-84.6	41.3	70	-82.75	40.89	131	-81.48	40.24
10	-84.48	40.04	71	-83.26	38.63	132	-83.09	40.98
11	-82.86	41.39	72	-83.33	39.39	133	-83.25	40.52
12	-81.89	39.37	73	-82.06	40.09	134	-81.66	40.05
13	-82.85	40.9	74	-83.19	38.86	135	-84	38.84
14	-83.27	41.29	75	-82.9	41.08	136	-81.25	39.65
15	-81.3	39.92	76	-82.19	40.29	137	-83.38	39.13
16	-83.8	39.34	77	-80.71	40.69	138	-82.08	40.99
17	-83.58	40.02	78	-81.61	40.68	139	-82.8	38.96
18	-81.82	39.11	79	-80.78	40.64	140	-82.13	40.68
19	-82.29	39.69	80	-84.66	40.66	141	-82.38	40.59
20	-83.32	39.08	81	-80.54	41.31	142	-82	39.46
21	-82.01	40.77	82	-82.63	39.18	143	-81.25	40.23
22	-83.54	38.71	83	-81.31	39.82	144	-83.72	38.8
23	-82.83	39.68	84	-81.05	40.19	145	-80.67	41.76
24	-82.87	39.13	85	-83.7	41.29	146	-84.23	41.09
25	-83.44	39.31	86	-83.19	40.39	147	-81.71	39.73
26	-82.47	39.36	87	-83.8	39.25	148	-81.65	39.47
27	-84.43	40.41	88	-83.16	41.2	149	-83.15	39.09
28	-81.13	39.83	89	-83.38	38.82	150	-82.58	39.55
29	-83.53	40.16	90	-82.18	39.54	151	-82.98	41.26
30	-81.97	40.36	91	-83.85	40.78	152	-82.17	39.15
31	-83.68	39.3	92	-81.01	39.7	153	-83.16	39.53
32	-81.58	40.39	93	-82.47	39.5	154	-82.61	40.27
33	-83.04	41.21	94	-82.34	39.1	155	-81.72	40.37
34	-84.11	40.01	95	-83.51	41.02	156	-82.51	38.56
35	-80.95	40.15	96	-83.55	40.34	157	-82.14	40.86
36	-83.35	41.6	97	-83.82	39.79	158	-81.08	41.26
37	-82.02	40.68	98	-83.68	39.08	159	-80.78	41.46
38	-84.13	38.89	99	-81.78	39.91	160	-81.73	40.18
39	-83.66	40.38	100	-81.59	39.87	161	-84.39	40.74
40	-83.03	39.13	101	-82.38	40.72	162	-80.96	40.41
41	-83.59	39.84	102	-84.71	41.38	163	-82.14	40.45

42	-81.84	40.37	103	-82	39.38	164	-80.66	41.27
43	-81.71	39.82	104	-83.73	40.47	165	-80.95	40.59
44	-84.56	39.59	105	-81.94	39.74	166	-84.43	40.63
45	-83.9	40.55	106	-80.95	41.63	167	-81.25	40.54
46	-82.31	40.67	107	-83.68	39.39	168	-80.88	40.68
47	-80.64	41.54	108	-84.26	40.63	169	-83.73	39.21
48	-82	39.59	109	-84.03	40.6	170	-82.12	39.69
49	-84.73	39.74	110	-81.07	40.46	171	-83.9	40.42
50	-82.45	41.31	111	-84.12	40.1	172	-83.32	40.8
51	-84.29	40.95	112	-80.83	40.77	173	-80.78	41.58
52	-84.43	40.5	113	-84.72	40.22	174	-83.75	41.06
53	-82.02	40.54	114	-83.38	39.04	175	-82.28	39.05
54	-84.72	40.31	115	-81.77	40.09	176	-84.6	40.18
55	-83.38	38.95	116	-81.24	40.65	177	-81.78	40.73
56	-81.89	39.91	117	-81.66	40.31	178	-84.61	41.53
57	-82.25	39.91	118	-84.56	41.67	179	-80.96	41.53
58	-82.35	39.41	119	-81.78	39.69	180	-83.28	41.02
59	-84.76	41.02	120	-84.12	41.32	181	-82.66	41.16
60	-81.88	39.46	121	-80.78	40	182	-80.6	40.91
61	-82.34	38.79	122	-82.37	40.36			

PA:

Station Number	Longitude	Latitude	Station Number	Longitude	Latitude	Station Number	Longitude	Latitude
1	-70.6	40.43	8	-72.85	40.68	15	-71.67	41.11
2	-72.46	40.2	9	-71.95	40.13	16	-73.14	41.24
3	-71.22	41.48	10	-71.6	41.36	17	-71.95	40.24
4	-71.69	40.22	11	-73.44	39.94	18	-71.71	41.39
5	-72.42	40.28	12	-73.3	39.94	19	-70.09	41.89
6	-72.22	41.02	13	-71.25	41.12			
7	-70.36	39.75	14	-71.99	41.24			

UT:

Station Number	Longitude	Latitude	Station Number	Longitude	Latitude	Station Number	Longitude	Latitude
1	-112.46	38.28	34	-111.92	38.42	67	-113.3	38.44
2	-110.88	40.77	35	-112.74	40.3	68	-111.29	41.5
3	-112.75	40.47	36	-110.09	37.62	69	-111.7	38.56
4	-111.77	41.62	37	-111.65	40.45	70	-111.53	38.52
5	-110.85	40.84	38	-112.32	39.45	71	-111.41	41.49
6	-111.97	38.29	39	-110.45	40.19	72	-112.28	40.02
7	-111.21	41.51	40	-110.31	37.8	73	-110.59	40.3
8	-109.93	37.18	41	-109.7	40.89	74	-109.91	37.59
9	-110.72	40.26	42	-109.97	37.61	75	-110.91	39.49
10	-109.95	37.41	43	-112.75	40.4	76	-112.46	39.29
11	-110.5	40.18	44	-112.37	38.29	77	-112.28	39.52
12	-112.72	37.23	45	-114.05	38.95	78	-112.66	40.71
13	-110.21	37.67	46	-109.92	37.24	79	-112.69	37.66
14	-112.29	41.67	47	-114.03	39.03	80	-110.14	37.66
15	-112.53	38.25	48	-111.93	41.91	81	-111.02	40.48
16	-112.72	40.59	49	-112.69	40.64	82	-110.26	37.73
17	-110.85	40.98	50	-109.91	37.45	83	-114.01	38.89
18	-112.38	38.24	51	-112.24	38.26	84	-113	39.19
19	-113.09	38.42	52	-113.96	38.78	85	-110.4	39.48
20	-110.21	37.43	53	-112.31	38.14	86	-110.69	40.19
21	-112.32	40.06	54	-113.99	38.83	87	-111.07	39.21
22	-111.06	40.52	55	-111.6	41.6	88	-111.44	40.57
23	-111.1	39.29	56	-112.69	38.08	89	-109.88	37.15
24	-111.43	38.64	57	-109.93	37.3	90	-111.24	39.65
25	-112.39	40.08	58	-112.74	40.54	91	-113.16	41.83
26	-110.92	40.47	59	-109.9	37.52	92	-112.28	39.67
27	-111	39.48	60	-112.01	38.2	93	-110.04	37.59
28	-111.77	38.51	61	-110.85	40.46	94	-111.67	40.96
29	-112.77	37.27	62	-110.34	37.86	95	-111.46	38.6

30	-113.12	41.97	63	-111.4	38.7	96	-109.35	37.34
31	-112.8	39.3	64	-113.83	38.6	97	-111.59	40.85
32	-111.17	39.54	65	-112.38	38.98	98	-111.9	40.94
33	-111.57	38.48	66	-113.9	38.69			

VA:

Station Number	Longitude	Latitude	Station Number	Longitude	Latitude	Station Number	Longitude	Latitude
1	-77.85	37.06	19	-79.3	37.96	37	-80.26	37.57
2	-78.73	37.64	20	-79.16	37.83	38	-79.87	38.12
3	-79.71	38.31	21	-78.7	36.85	39	-81.16	37.26
4	-76.92	38.19	22	-80.12	37.51	40	-78.6	38.68
5	-78.04	39.18	23	-77.66	38.63	41	-78.27	38.3
6	-77.66	36.76	24	-77.28	36.78	42	-80.12	36.79
7	-75.83	37.52	25	-79.54	37.5	43	-80.32	37.39
8	-81.6	37.08	26	-76.89	37.69	44	-81.96	36.89
9	-77.17	37.85	27	-79.33	37.67	45	-81.3	37.04
10	-79.95	38.02	28	-80.56	36.66	46	-78.71	36.72
11	-82.54	37.11	29	-77.14	36.87	47	-78.73	37.07
12	-80.21	36.86	30	-77.04	37.79	48	-79.24	36.72
13	-79.79	38.21	31	-79.24	36.82	49	-78.27	38.45
14	-81.45	36.96	32	-79.03	37.89	50	-80.95	37.27
15	-79.41	37.56	33	-78.21	36.55	51	-80.07	37.18
16	-77.01	37.13	34	-80.16	37.64	52	-79.65	38.45
17	-78.32	37	35	-79.71	37.45			
18	-78.88	38.01	36	-81.5	36.62			

WI:

Station Number	Longitude	Latitude	Station Number	Longitude	Latitude	Station Number	Longitude	Latitude
1	-90.22	43.28	21	-88.78	44.8	41	-90.43	43.54

2	-88.93	46.03	22	-90.4	46.36	42	-91.16	44.1
3	-88.34	43.89	23	-89.09	45.21	43	-92.34	45.64
4	-90.09	46.03	24	-88.75	44.94	44	-92.18	45.63
5	-89.38	43	25	-89.35	43.57	45	-90.87	43.12
6	-88.66	43.36	26	-91.98	46.18	46	-89.9	42.59
7	-91.93	44.79	27	-90.64	43.51	47	-88.83	45.91
8	-88.77	45.38	28	-91.11	43.56	48	-90.33	43.18
9	-89.93	45.15	29	-90.25	44.35	49	-88.18	43.69
10	-88.52	45.92	30	-90.08	43.02	50	-89.19	42.83
11	-89.9	46.3	31	-92.69	45.55	51	-88.76	45.15
12	-89.12	45.09	32	-91.49	44.43	52	-88.63	45.02
13	-88.82	45.78	33	-89.44	43.79	53	-88.93	45.05
14	-91.22	45.74	34	-89.82	42.92	54	-90.41	46.46
15	-91.75	44.22	35	-90.04	42.87	55	-91.22	45.61
16	-91.8	44.7	36	-90.86	43.26	56	-89.5	43.25
17	-90.59	44.72	37	-89.43	45.9	57	-89.26	44.5
18	-92.56	45.46	38	-91.04	43.15	58	-90.85	46.56
19	-89.11	43.5	39	-90.59	46.38	59	-89.87	43.04
20	-88.92	44.46	40	-88.91	45.26			

Appendix B – Location Plan for Adding New Stations in Existing RWIS Network

Table 5: Locations of 10 and 20 additional RWIS stations considering (a) weather data only and (b) dual criteria (both weather and traffic data)

CA

Station Number	Weather Only		Dual Criteria	
	Longitude	Latitude	Longitude	Latitude
1	-120.04	35.35	-119.81	37.75
2	-122.43	40.23	-117.23	34.34
3	-121.98	37.32	-119.86	37.26
4	-117.35	34.01	-122.86	39.73
5	-116.99	32.68	-118.2	36.03
6	-121.4	39.82	-121.58	40.33
7	-117.39	36.34	-121.59	37.36
8	-120.56	37.33	-122.69	41.27
9	-117.65	33.98	-122.93	39.79
10	-121.47	36.52	-120.27	36.95
11	-121.95	38.42	-121.67	38.23
12	-118.29	33.82	-115.44	33.84
13	-116.40	33.65	-119.67	37.85
14	-121.23	36.63	-122.81	39.68
15	-121.73	39.66	-119.38	37.34
16	-119.41	34.34	-122.42	39.8
17	-118.00	34.70	-119.45	37.15
18	-117.63	34.14	-119.64	37.53
19	-116.51	33.12	-118.78	36.54
20	-122.50	37.70	-119.49	37.81

CO

Station Number	Weather Only		Dual Criteria	
	Longitude	Latitude	Longitude	Latitude
1	-104.73	40.58	-107.55	38.56
2	-104.50	40.12	-108.48	38.95
3	-107.30	38.08	-103.78	40.61
4	-108.76	37.59	-106.32	37.1
5	-108.53	37.46	-105.61	40.39
6	-104.73	38.23	-103.18	38.45
7	-107.89	38.47	-104.26	40.08
8	-104.79	39.59	-102.23	40.91
9	-105.48	38.14	-103.89	37.05
10	-105.72	39.76	-103.83	37.78
11	-106.83	39.66	-102.87	39.25
12	-102.07	40.59	-104.62	37.69
13	-105.90	40.17	-105.6	39.04
14	-107.69	37.75	-106.04	37.28
15	-105.49	39.41	-106.2	40.66
16	-102.30	40.55	-105.43	38.55
17	-105.14	37.56	-105.53	37.15
18	-103.72	40.61	-104.55	40.62
19	-102.30	40.68	-102.13	40.58
20	-105.60	39.67	-108.95	37.9

DE

Station Number	Weather Only		Dual Criteria	
	Longitude	Latitude	Longitude	Latitude
1	-75.65	39.24	-75.3	38.65
2	-75.54	39.20	-75.65	39.24
3	-75.65	39.15	-75.47	38.7
4	-75.30	38.61	-75.65	39.15
5	-75.36	38.70	-75.36	38.52
6	-75.59	38.74	-75.65	38.79
7	-75.60	39.64	-75.77	39.42
8	-75.66	38.83	-75.71	38.97
9	-75.36	38.52	-75.19	38.52
10	-75.59	38.61	-75.6	39.06
11	-75.47	38.61	-75.59	38.61
12	-75.47	38.48	-75.37	38.92
13	-75.77	39.41	-75.19	38.65
14	-75.59	39.10	-75.47	38.88
15	-75.42	38.92	-75.36	38.7
16	-75.65	38.52	-75.47	38.61
17	-75.19	38.74	-75.71	38.83
18	-75.72	39.51	-75.54	39.34
19	-75.66	39.73	-75.76	39.2
20	-75.18	38.52	-75.65	38.52

IA

Station Number	Weather Only		Dual Criteria	
	Longitude	Latitude	Longitude	Latitude
1	-92.53	41.75	-95.68	42.27
2	-94.98	41.38	-92.06	40.85
3	-95.70	41.23	-90.85	41.69
4	-91.19	42.24	-91.13	42.42
5	-94.23	42.74	-95.38	40.88
6	-91.09	41.43	-92.16	42.61
7	-91.92	42.47	-95.53	41.64
8	-93.80	42.30	-94.01	40.72
9	-93.43	41.67	-92.03	43.06
10	-92.83	41.04	-93.37	41.89
11	-95.47	41.50	-91.01	42.15
12	-95.06	41.52	-95.85	42.13
13	-91.01	42.29	-95.04	41.38
14	-92.03	43.06	-91.76	41.17
15	-95.83	42.98	-93.25	41.76
16	-91.63	41.48	-92.16	41.76
17	-96.14	42.85	-91.54	42.88
18	-93.39	43.15	-91.28	43.36
19	-95.37	42.01	-95.94	41.68
20	-91.92	41.80	-94.31	40.71

IL

Station Number	Weather Only		Dual Criteria	
	Longitude	Latitude	Longitude	Latitude
1	-90.67	40.69	-89.11	37.15
2	-91.13	39.92	-89.18	40.05
3	-88.68	37.43	-88.46	40.57
4	-89.72	38.31	-88.21	40.8
5	-88.45	40.11	-88.21	40.93
6	-88.29	37.46	-90.62	39.33
7	-88.62	41.51	-88.27	37.48
8	-89.05	41.51	-90.4	40.79
9	-90.11	42.03	-90.54	40.73
10	-89.47	37.56	-90.01	41
11	-88.34	39.05	-89.33	37.62
12	-87.69	41.61	-90.06	41.56
13	-90.98	40.67	-88.59	40.48
14	-87.73	41.04	-88.82	40.51
15	-89.88	38.53	-89.24	38.39
16	-87.93	38.39	-88.48	37.63
17	-89.23	38.32	-90.71	40.23
18	-89.11	38.62	-89.87	40.93
19	-89.61	40.81	-90.87	40.97
20	-90.18	38.59	-89.71	41.56

KS

Station Number	Weather Only		Dual Criteria	
	Longitude	Latitude	Longitude	Latitude
1	-96.90	38.81	-99.76	37.44
2	-96.87	39.84	-96.33	39.7
3	-95.68	37.69	-97.36	38.68
4	-95.21	39.22	-97.93	39.68
5	-94.95	38.62	-101.18	38.99
6	-95.13	39.57	-96.97	39.63
7	-100.12	38.64	-101.72	39.61
8	-97.64	39.00	-101.27	38.13
9	-98.74	38.15	-98.47	37.47
10	-94.95	37.72	-101.76	37.49
11	-100.49	39.58	-97.58	39.11
12	-95.36	38.55	-94.83	37.6
13	-95.69	38.64	-101.23	38.9
14	-98.86	38.87	-101.3	39.03
15	-95.76	37.20	-101.69	37.26
16	-96.96	38.67	-100.7	38.05
17	-96.26	38.88	-101.27	38.27
18	-101.76	39.33	-101.85	39.83
19	-97.33	37.51	-95.31	39.68
20	-100.83	39.44	-95.27	39.81

MI

Station Number	Weather Only		Dual Criteria	
	Longitude	Latitude	Longitude	Latitude
1	-84.93	43.41	-87.49	45.88
2	-86.25	43.24	-85.09	43.31
3	-83.75	42.50	-85	42.57
4	-85.72	43.61	-87.22	46.16
5	-85.65	43.02	-88.06	47.47
6	-84.60	43.39	-89.57	46.71
7	-85.23	42.36	-85.85	43.79
8	-84.73	45.45	-83.77	43.48
9	-85.41	41.98	-83.84	45.99
10	-83.36	42.04	-84.16	45.08
11	-84.22	42.29	-86.77	46.34
12	-84.11	44.38	-83.68	43.23
13	-85.34	43.43	-84.04	42.22
14	-83.33	43.34	-84.24	42.84
15	-83.75	42.35	-85.8	43.62
16	-84.50	46.27	-85.32	42.38
17	-84.36	45.36	-86.05	42.3
18	-83.87	43.59	-84.21	45.22
19	-84.26	43.66	-84.61	44.13
20	-85.53	43.68	-86.22	44.69

MN

Station Number	Weather Only		Dual Criteria	
	Longitude	Latitude	Longitude	Latitude
1	-91.75	46.98	-92.53	47.51
2	-93.65	44.67	-93.46	44.94
3	-94.76	47.60	-93.29	44.8
4	-94.84	46.33	-93.45	45.1
5	-95.17	43.81	-93.06	45.04
6	-94.30	44.85	-93.09	44.97
7	-96.49	46.50	-93.07	44.88
8	-92.90	44.07	-92.89	47.45
9	-95.65	45.31	-93.28	43.92
10	-95.28	45.50	-96.76	46.84
11	-95.88	46.77	-95.74	45.11
12	-94.61	43.64	-96.18	45.23
13	-95.53	44.80	-95.00	45.89
14	-93.91	46.48	-95.94	44.12
15	-96.46	48.60	-91.82	43.79
16	-93.90	45.59	-95.51	45.7
17	-94.22	45.50	-95.97	44.79
18	-95.03	45.12	-95.47	46.33
19	-94.74	43.69	-96.42	46.13
20	-93.45	45.00	-95.48	45.03

ND

Station Number	Weather Only		Dual Criteria	
	Longitude	Latitude	Longitude	Latitude
1	-98.34	48.03	-99.22	47.15
2	-98.69	46.63	-103.89	48.03
3	-99.74	47.44	-97.94	46.11
4	-100.96	48.06	-104	47.16
5	-100.01	47.44	-103.59	48.58
6	-99.63	48.52	-103.16	46.52
7	-97.20	48.15	-97.84	46.63
8	-100.25	46.27	-103.46	48.58
9	-97.13	46.26	-99.62	48.69
10	-98.94	48.79	-98.7	47.23
11	-102.28	46.86	-99.33	46.53
12	-100.88	47.84	-103.62	48.8
13	-100.72	46.71	-99.35	46.38
14	-100.50	46.31	-100.91	47.61
15	-103.62	48.57	-103.65	46.23
16	-98.87	48.16	-101.54	47.86
17	-99.41	47.49	-102.87	46.13
18	-99.94	47.76	-103.14	48.05
19	-98.35	47.80	-99.62	48.47
20	-101.72	48.46	-103.87	48.61

OH

Station Number	Weather Only		Dual Criteria	
	Longitude	Latitude	Longitude	Latitude
1	-84.12	40.06	-83.58	41.28
2	-82.79	40.80	-82.02	40.54
3	-84.61	41.57	-83.72	38.81
4	-83.07	40.35	-80.77	41.58
5	-82.06	39.96	-82.35	39.41
6	-83.45	39.22	-81.36	39.74
7	-82.84	40.67	-84.72	41.52
8	-81.85	41.13	-83.72	40.25
9	-82.02	40.68	-81.19	41.49
10	-84.10	40.82	-80.96	41.41
11	-81.61	40.86	-83.56	40.79
12	-81.37	40.73	-81.01	40.01
13	-82.14	40.68	-84.43	40.41
14	-83.07	40.26	-81.65	39.73
15	-81.90	40.77	-82.92	41.12
16	-82.65	39.95	-83.92	40.96
17	-83.91	40.42	-81.77	39.69
18	-83.65	40.11	-80.95	41.63
19	-82.67	40.85	-81.42	39.82
20	-80.59	41.04	-81.95	39.6

PA

Station Number	Weather Only		Dual Criteria	
	Longitude	Latitude	Longitude	Latitude
1	-79.13	40.06	-73.14	41.24
2	-77.28	40.13	-73.63	39.72
3	-79.60	41.60	-72.7	40.8
4	-80.22	39.90	-71.89	41.33
5	-77.50	41.03	-70.09	39.86
6	-76.46	40.52	-71.61	41.11
7	-75.54	40.05	-71.49	40.15
8	-75.51	40.41	-72.46	41.71
9	-77.89	40.10	-72.01	40.35
10	-77.33	39.76	-72.4	40.21
11	-76.80	40.16	-72.67	40.3
12	-80.38	40.98	-73.22	41.59
13	-77.60	39.73	-72.17	40.96
14	-75.82	40.78	-71.68	41.43
15	-78.35	40.51	-71.79	39.86
16	-75.49	40.15	-71.28	40.25
17	-74.92	40.25	-72.98	41.34
18	-79.07	41.33	-71.17	41.44
19	-79.51	40.33	-71.08	39.91
20	-77.88	42.00	-72.54	40.86

UT

Station Number	Weather Only		Dual Criteria	
	Longitude	Latitude	Longitude	Latitude
1	-111.89	41.25	-109.92	37.18
2	-113.86	41.42	-110.89	40.76
3	-112.31	40.35	-109.94	37.6
4	-112.59	37.75	-111.51	38.54
5	-113.18	40.73	-114.03	39.02
6	-112.50	37.51	-112.45	39.28
7	-112.37	39.52	-112.73	40.56
8	-109.12	37.18	-112.69	38.08
9	-111.09	41.78	-112.36	38.24
10	-111.88	39.50	-112.72	37.66
11	-109.32	40.17	-109.91	37.24
12	-111.25	39.65	-112.31	38.14
13	-112.74	40.51	-114.03	38.96
14	-111.76	41.25	-110.86	40.83
15	-112.06	41.12	-111.23	41.51
16	-111.53	39.95	-111.67	40.96
17	-111.67	39.23	-110.71	37.64
18	-112.03	40.70	-109.9	37.48
19	-110.83	39.61	-109.87	37.15
20	-111.48	40.44	-109.89	37.54

VA

Station Number	Weather Only		Dual Criteria	
	Longitude	Latitude	Longitude	Latitude
1	-79.09	38.15	-78.79	38.38
2	-76.43	36.78	-79.24	37.82
3	-78.69	37.18	-80.63	37.23
4	-77.01	37.82	-81.69	37.04
5	-79.22	37.91	-81.79	37.29
6	-78.00	39.12	-80.17	36.88
7	-77.31	38.59	-77.03	37.12
8	-76.16	36.82	-79.43	37.56
9	-76.42	37.67	-79.93	38.05
10	-78.29	38.00	-79.54	37.49
11	-76.70	37.07	-79.07	37.86
12	-77.36	37.74	-78.72	36.73
13	-78.92	38.15	-77.83	37.06
14	-77.61	37.06	-78.94	37.94
15	-77.52	36.68	-79.77	38.24
16	-80.13	37.10	-79.33	37.65
17	-76.71	37.28	-80.33	37.39
18	-79.52	37.34	-78.17	38.71
19	-80.24	37.21	-82.85	36.92
20	-80.21	36.74	-78.7	36.85

WI

Station Number	Weather Only		Dual Criteria	
	Longitude	Latitude	Longitude	Latitude
1	-89.70	43.12	-89.94	42.62
2	-91.46	44.57	-90.33	43.56
3	-88.33	43.42	-90.67	43.19
4	-89.18	42.75	-89.07	45.1
5	-90.47	42.74	-90.86	43.14
6	-88.01	43.66	-92.56	45.53
7	-91.98	44.66	-90.39	46.37
8	-88.26	44.62	-90.07	43.05
9	-91.11	45.72	-92.24	45.36
10	-89.88	44.34	-90.12	45.42
11	-89.65	44.84	-91.81	44.69
12	-90.25	44.02	-92.27	45.64
13	-88.70	43.81	-90.71	43.83
14	-88.88	43.86	-90.34	43.17
15	-90.61	43.34	-88.57	44.6
16	-90.04	43.42	-89.94	42.83
17	-89.91	43.71	-87.92	45.75
18	-92.00	45.64	-91.68	44.41
19	-88.15	42.69	-88.77	45.38
20	-92.38	45.72	-89.41	45.97